



Population-based gradient descent weight learning for graph coloring problems

Olivier Goudet, Béatrice Duval, Jin-Kao Hao

► To cite this version:

Olivier Goudet, Béatrice Duval, Jin-Kao Hao. Population-based gradient descent weight learning for graph coloring problems. Knowledge-Based Systems, 2021, 212, pp.106581 -. <10.1016/j.knosys.2020.106581>. <hal-03493613>

HAL Id: hal-03493613

<https://hal.science/hal-03493613v1>

Submitted on 2 Jan 2023

HAL is a multi-disciplinary open access archive for the deposit and dissemination of scientific research documents, whether they are published or not. The documents may come from teaching and research institutions in France or abroad, or from public or private research centers.

L'archive ouverte pluridisciplinaire **HAL**, est destinée au dépôt et à la diffusion de documents scientifiques de niveau recherche, publiés ou non, émanant des établissements d'enseignement et de recherche français ou étrangers, des laboratoires publics ou privés.



Distributed under a Creative Commons CC BY-NC 4.0 - Attribution - Non-commercial use - International License

Population-based Gradient Descent Weight Learning for Graph Coloring Problems

Olivier Goudet ^a, Béatrice Duval ^a, Jin-Kao Hao ^{a,b,*}

^a*LERIA, Université d'Angers, 2 Boulevard Lavoisier, 49045 Angers, France*

^b*Institut Universitaire de France, 1 Rue Descartes, 75231 Paris, France*

Minor revision, 24 Oct. 2020 (Subm. April 2020, first rev. July 2020)

Abstract

Graph coloring involves assigning colors to the vertices of a graph such that two vertices linked by an edge receive different colors. Graph coloring problems are general models that are very useful to formulate many relevant applications and, however, are computationally difficult. In this work, a general population-based weight learning framework for solving graph coloring problems is presented. Unlike existing methods for graph coloring that are specific to the considered problem, the presented work targets a generic objective by introducing a unified method that can be applied to different graph coloring problems. This work distinguishes itself by its solving approach that formulates the search of a solution as a continuous weight tensor optimization problem and takes advantage of a gradient descent method computed in parallel on graphics processing units. The proposed approach is also characterized by its general global loss function that can easily be adapted to different graph coloring problems. The usefulness of the proposed approach is demonstrated by applying it to solve two typical graph coloring problems and performing large computational studies on popular benchmarks. Improved best-known results (new upper bounds) are reported for several large graphs.

Keywords: Learning-based problem solving; heuristics; gradient descent; combinatorial search problems; graph coloring.

* Corresponding author.

Email addresses: olivier.goudet@univ-angers.fr (Olivier Goudet),
beatrice.duval@univ-angers.fr (Béatrice Duval),
jin-kao.hao@univ-angers.fr (Jin-Kao Hao).

1 Introduction

Graph coloring problems are popular and general models that can be used to formulate numerous practical applications in various domains [27]. Given an undirected graph $G = (V, E)$ with a set of vertices V and a set of edges E , a legal coloring is a partition of vertex set V into k different color groups (also called independent sets) such that two vertices linked by an edge belong to different color groups. A legal coloring of G can also be defined by a mapping that associates each vertex to a color such that two adjacent vertices must receive different colors (this is the so-called graph coloring constraint). Typically, the used colors or the color groups are represented by consecutive integers $1, \dots, k$. Consequently, the following statements are equivalent: vertex v is assigned to (or receives) color i ; v is assigned to color group i .

Graph coloring problems generally involve finding a *legal* coloring of a graph while considering some additional decision criteria and constraints. Specifically, the popular Graph Coloring Problem (GCP) is to determine the chromatic number of a graph, i.e., the smallest number of colors needed to reach a legal coloring of the graph. With an additional equity constraint, the Equitable graph Coloring problem (ECP) [34] requires finding a legal coloring with the minimum number of colors while the sizes of the color groups differ by at most one (i.e., the color groups are almost of the same size). When the number of colors k is given, the Graph k -coloring Problem (k -COL) is to find a legal coloring of a graph with the k given colors.

In terms of computational complexity, graph coloring problems including those mentioned above are NP-hard and thus computationally challenging. Given their theoretical and practical significance, graph coloring problems have been studied very intensively in the literature. However, as the review on the GCP and the ECP of Section 2 shows, studies on graph coloring are usually specific to a problem and it is difficult to generalize a method designed for a coloring problem to other coloring problems even if they are tightly related.

This work aims to target a more general objective for solving graph coloring problems by proposing a framework that can be applied to different graph coloring problems and more generally grouping problems where a set of items needs to be separated into different groups according to some given grouping constraints and objectives. The contributions of this work are summarized as follows.

First, a population-based gradient descent weight learning approach with a number of original features is proposed. A coloring problem is considered from the perspective of continuous optimization to benefit from the powerful gradient descent. Specifically, a weight matrix representation of a candidate coloring

is used, where each entry of the matrix corresponds to a learned propensity of a vertex to receive a particular color. Then a gradient descent method is used to improve a population of candidate solutions (or individuals) by minimizing a global loss function. The global loss function is designed to effectively guide the gradient descent. To be informative, the global loss function aggregates different terms: a fitness term measuring the quality of a candidate solution, a penalization term aiming to discourage the individuals to repeat the same color assignment mistakes and a bonus term aiming to encourage the individuals to keep the shared correct assignments. To solve this problem, the tensor of candidate solutions is expressed as a tensor of continuous weight matrices. Accelerated training with Graphics Processing Unit (GPU) is used to deal with multiple parallel solution evaluations. As the first study of using gradient descent based weight learning to solve graph coloring problems with tensor calculations, this work enriches the still limited toolkit of general solution methods for this important class of problems.

Secondly, the usefulness of the proposed framework is demonstrated by applying it to two popular graph coloring problems: the GCP and the ECP. For both problems, extensive computational experiments are presented on well-known benchmark graphs and show the competitiveness of our approach compared to state-of-the-art algorithms. In particular, improved best results are presented for several large geometric graphs and large random graphs for the ECP.

Thirdly, this work shows the viability of formulating a discrete graph coloring problem as a real-valued weight learning problem. The competitive results on two challenging representative graph coloring problems invite more investigations of testing the proposed approach to other graph coloring problems and related grouping problems.

The rest of the paper is organized as follows. Section 2 reviews related heuristics for the GCP and the ECP. Section 3 describes the proposed approach and its ingredients. Section 4 provides illustrative examples on the gradient descent learning. Section 5 reports computational results on well-known benchmark graphs and shows comparisons with the state-of-the-art. Section 6 discusses the applicability of the proposed framework to other graph problems. Section 7 summarizes the contributions and presents perspectives for future work.

2 Reference heuristics for the two coloring problems

The GCP and the ECP have been studied very intensively in the past. Both problems are known to be NP-hard in the general case (see [20] for the GCP and [16] for the ECP). Thus, assuming that $N \neq NP$, no algorithm can solve these problems exactly in polynomial time except for specific cases. In practice,

78 there are graphs with some 250 vertices that cannot be solved optimally by
79 any existing exact algorithm (see [31] for the GCP and [33] for the ECP).

80 Therefore, to handle large graphs, heuristics are typically used to solve these
81 problems approximately. Generally, heuristics proceed by successively solv-
82 ing the k -coloring problem with decreasing values of k [17] and the smallest
83 possible k gives an upper bound of the optimum.

84 A thorough review of existing heuristics for the GCP and the ECP is out
85 of the scope of this work. Instead, a brief description of the main heuristics
86 including in particular the best-performing heuristics is presented below. For a
87 comprehensive review of these problems, the reader is referred to the following
88 references for the GCP: local search heuristics [19], exact algorithms [32] and
89 new developments on heuristics till 2013 [17]. For the ECP, both [40] and [42]
90 provide a brief review of main heuristic algorithms.

91 2.1 Heuristics for the graph coloring problem

92 There are different ways of classifying for the GCP. Following [17], these heuris-
93 tics can be classified in three main categories: local search based methods,
94 hybrid methods combining population-based genetic search and local search,
95 and large independent set extraction.

96 Local search heuristics iteratively improve the current solution by local mod-
97 ifications (typically, change the color of a vertex) to optimize a cost function,
98 which typically corresponds to the number of conflicting edges (i.e., edges
99 whose endpoints being assigned the same color). To be effective, a local search
100 heuristics usually integrate different mechanisms to escape local optima traps.
101 One of the most popular local search heuristics for the GCP is the *TabuCol* al-
102 gorithm [22]. *TabuCol* iteratively makes transitions from the current solution
103 to a new (neighbor) solution by changing the color of an endpoint of a conflict-
104 ing edge according to a specific rule. In order to avoid search cycling, it uses a
105 special memory (called tabu list) to prevent a vertex from receiving its former
106 color. Despite its simplicity, *TabuCol* performs remarkably well on graphs of
107 reasonable sizes (with less than 500 vertices). This algorithm was largely used
108 as the key local optimization component of several state-of-the-art hybrid al-
109 gorithms (see below). Recently, *TabuCol* has also been adopted as the local
110 optimizer of the probability based learning local search method (PLSCOL)
111 [44]. Finally, this single trajectory local search approach has been extended
112 to multiple trajectory local search, which is exemplified by the Quantum An-
113 nealing algorithm (QA) [41]. In QA, n candidate solutions are optimized by a
114 simulating annealing algorithm, while the interactions between the solutions
115 occur through a specific pairwise attraction process, encouraging the solutions

116 to become similar to their neighbors and improving the spreading of good so-
117 lution features among new solutions.

118 The second category of methods includes hybrid algorithms, in particular,
119 based on the *memetic* framework [36]. These hybrid algorithms combine the
120 benefits of local search for intensification with a population of high-quality
121 solutions offering diversification possibilities. Different solutions evolve sepa-
122 rately using a local search algorithm, such as the above-mentioned *TabuCol*
123 algorithm, and a crossover operator is used to create new candidate solutions
124 from existing solutions. One of the most popular crossover operators for the
125 GCP is the Greedy Partition Crossover (GPX) introduced in the hybrid evo-
126 lutionary algorithm (HEA) [18]. HEA follows the idea of grouping genetic
127 algorithms [13] and produces offspring by choosing alternatively the largest
128 color class in the parent solutions. The MMT algorithm [30] completes a first
129 phase of optimization with a *memetic* algorithm by a second phase of opti-
130 mization based on the set covering formulation of the problem and using the
131 best independent sets found so far. An extension of the HEA algorithm called
132 MACOL (denoted as MA in this paper) was proposed in [28]. It introduces a
133 new adaptive multi-parent grouping crossover (AMPaX) and a new distance-
134 and-quality based replacement mechanism used to maintain the diversity of
135 the solutions in the population. Recently, a very powerful variation of the
136 HEA algorithm, called hybrid evolutionary algorithm in duet (HEAD), was
137 proposed in [35], which relies on a population of only two solutions. In order
138 to prevent a premature convergence, HEAD introduces an innovative diversi-
139 fication strategy based on an archive of elite solutions. The idea is to record
140 the best solutions (elite solutions) obtained in previous few generations and
141 to reintroduce them in the population when the two solutions becomes too
142 similar.

143 The third category of approaches is based on extracting large independent
144 sets in order to copy with the difficulty of coloring very large graphs [43].
145 With this approach, an independent set algorithm is used to identify as many
146 possible independent sets of large sizes and a coloring algorithm is employed
147 to color the residual graphs (whose size is largely reduced). These methods
148 are particularly effective to color large graphs with at least 1000 vertices.

149 One notices that the above algorithms cover the current best-known results
150 on the benchmark instances used in the experimental section of this work.
151 However, no single algorithm is able to reach the best-known results for these
152 hard instances. Moreover, it is worth mentioning that most current best-known
153 results have not been updated for a long time, indicating the high difficulty
154 of further improving these results.

155 Finally, it is worth mentioning that there are a number of other algorithms
156 based on fashionable metaheuristics including ant colony optimization [9], par-

157 ticle swarm optimization [2], and other fanciful bio-inspired methods (flower
 158 pollination [5], firefly [10] and cuckoo optimization [29]). However, the com-
 159 putational results reported by these algorithms (often on easy benchmark
 160 instances only) show that they are not competitive at all compared to the
 161 state-of-the-art coloring algorithms.

162 2.2 Heuristics for the equitable graph coloring problem

163 Most of the above-mentioned best performing methods for the GCP rely in one
 164 way or another on extraction of large independent sets or spreading of large
 165 building blocks between solutions. Thus, these methods cannot generally be
 166 applied as it stands for the ECP, because regrouping vertices in large sets may
 167 conflict with the equity constraint. Therefore different approaches have been
 168 proposed in the literature for the ECP.

169 One of the first method is the tabu search algorithm TabuEqCol [12], which
 170 is an adaptation of the popular *TabuCol* algorithm designed for the GCP [22]
 171 to the ECP. This algorithm was improved in [25] by the backtracking based
 172 iterated tabu search (BITS), which embeds a backtracking scheme under the
 173 iterated local search framework. These two algorithms only consider feasible
 174 solutions with respect to the equity constraint, which may restrict the explo-
 175 ration of the space search too much.

176 A new class of methods relaxes the equity constraint and considers both
 177 equity-feasible and equity-infeasible solutions to facilitate the transition be-
 178 tween visiting structurally different solutions. By enlarging their search spaces,
 179 these algorithms are able to improve on the results reported by the basic tabu
 180 search algorithm [12] and the backtracking based iterated tabu search algo-
 181 rithm [25]. The first work in this direction is the Feasible and Infeasible Search
 182 Algorithm (FISA) [39]. The hybrid tabu search (HTS) algorithm [42] is an-
 183 other important algorithm exploring both equity-feasible and equity-infeasible
 184 solutions and applying an additional novel cyclic exchange neighborhood. Fi-
 185 nally, the latest memetic algorithm (MAECP) [40] is a population-based hy-
 186 brid algorithm combining a backbone crossover operator, a two-phase feasible
 187 and infeasible local search and a quality-and-distance pool updating strategy.
 188 MAECP has reported excellent results on the set of existing benchmark in-
 189 stances in the literature. Among the algorithms, FISA, HTS and in particular
 190 MAECP hold the current best-known results on the benchmark instances used
 191 in the experiments of this work.

192 The above review indicates that the existing approaches for the GCP and the
 193 ECP are specific (i.e., they are specially designed for the given problem) and
 194 thus cannot be applied to other (even tightly related) coloring problems. For

instance, the best performing methods for the GCP such as the multi-parent memetic algorithm [28], the two phase memetic algorithm [30] and the two individual memetic algorithm [35] are based on specific crossover operators to combine large color classes. Such a strategy is meaningful for the GCP, but becomes inadequate for the ECP due to the equity constraint. As such, these approaches lack generality and are not readily applicable to other problems.

The current work aims to propose a more flexible and general framework for graph coloring problems, which is less dependent on the type of coloring problems or the type of graphs. This goal is achieved by formulating the computation of a solution of a coloring problem as a weight tensor optimization problem, which is solved by a first order gradient descent. As such, this approach can benefit from GPU accelerated training to deal with multiple parallel solution evaluations, ensuring a large examination of the given search space. As the computational results presented in Section 5 show, this unified approach, with slight modifications, is able to compete favorably with state-of-the-art algorithms for both the GCP and the ECP, leading to record breaking results for several large graphs for the ECP. Generally, this work narrows the gap between discrete optimization and gradient descent based continuous optimization, the latter being routinely used in particular in machine learning to train deep neural networks with billion of parameters.

3 Population-based gradient descent learning for graph coloring

Given a graph $G = (V, E)$ with vertex set $V = \{v_i\}_{i=1}^n$ and edge set E , the considered problem is to partition V into a minimum number of k color groups g_i ($i = 1, \dots, k$), while satisfying some constraints. For the GCP, only the coloring constraint is imposed while for the ECP, the equity constraint must be additionally satisfied. To minimize the number of color groups, a typical approach is to solve a series of problems with different fixed k . For instance, the GCP can be approximated by solving a sequence of k -COL problems, i.e., finding k -colorings for decreasing k values [17] such that each k leading to a legal coloring is an upper bound of the chromatic number of the graph. This approach is adopted to handle both the GCP and the ECP in this work.

3.1 Tensor representation of a population of candidate solutions

A candidate solution for a graph coloring problem with k color groups can be represented by a binary matrix $S = \{s_{i,j}\}$ in $\{0, 1\}^{n \times k}$, with $s_{i,j} = 1$ if the i -th vertex v_i belongs to the color group j and $s_{i,j} = 0$ otherwise. Therefore, $\sum_{j=1}^k s_{i,j} = 1$, as one vertex belongs exactly to one color group. For

the two graph coloring problems considered in this work (GCP and ECP), the constraints and the optimization objective of each problem are formulated as the minimization of a single fitness function $f : \{0, 1\}^{n \times k} \rightarrow \mathbb{R}$. The goal of the problem is then to find a solution S such that $f(S)$ is minimum. The definition of this function for the GCP and the ECP is provided in Section 3.5.

In the proposed approach, a population of D candidate solutions (individuals) will be considered and their fitness scores will be computed in parallel with tensor calculus on Compute Unified Device Architecture (CUDA) for GPU hardware. In order to do that, the D matrices S_d ($d \in \llbracket 1, D \rrbracket$) of the population are regrouped in a single three-dimensional tensor $\mathbf{S} = \{s_{d,i,j}\}$ in $\{0, 1\}^{D \times n \times k}$. For a tensor \mathbf{S} of D candidate solutions, its *global fitness function* is defined by the sum of all individual fitness $\sum_{d=1}^D f(S_d)$ and will be written as $f(\mathbf{S})$.

Hereafter, **bold** symbols are used to denote three-dimensional tensors and normal symbols to represent the underlying two-dimensional matrices, just like tensor \mathbf{S} of D candidate solutions and a single solution matrix S .

3.2 Weight formulation of a coloring problem

Inspired by the works on reinforcement learning based local search [45] and ant colony optimization [11], a real-valued weight matrix $W = \{w_{i,j}\}$ in $\mathbb{R}^{n \times k}$ is employed. It is composed of n real numbers vectors w_i of size k corresponding to a learned propensity of each vertex v_i to receive a particular color. In order to build a discrete solution S from W , each vertex v_i will be assigned to the color group with the maximum weight in w_i .

As a main idea, a real-valued weight tensor $\mathbf{W} = \{w_{d,i,j}\}$ in $\mathbb{R}^{D \times n \times k}$ of D matrices W_d is used to compute a tensor \mathbf{S} of D discrete coloring solutions. This is simply achieved by a function $g : \mathbb{R}^{D \times n \times k} \rightarrow \{0, 1\}^{D \times n \times k}$ such that $\mathbf{S} = g(\mathbf{W})$ (cf. Section 3.4 below). As \mathbf{S} derives from \mathbf{W} , the given coloring problem becomes then the one of finding \mathbf{W} such that $f \circ g(\mathbf{W})$ is minimum.

Our approach starts with a random weight tensor \mathbf{W} where each entry is sampled independently from a normal distribution $\mathcal{N}(0, \sigma_0)$. Then, as explained below, a first order gradient descent is employed to update this weight tensor \mathbf{W} with information learned during the search.

264 The population-based gradient descent weight learning for graph coloring (or
 265 simply TensCol) proposed in this work relies on a population of candidate
 266 solutions represented as a weight tensor and performs tensor calculations in
 267 parallel with GPU by minimizing a flexible global loss function that encourages
 268 correction of wrong vertex-to-color assignments and consolidation of correct
 269 assignments of the solutions.

270 From the perspective of algorithmic procedure, the proposed TensCol algo-
 271 rithm iteratively improves its population in four steps, as illustrated by Figure
 272 1. First, given the weight tensor \mathbf{W} , the associated population of solutions \mathbf{S}
 273 (colorings) is computed (Step 1). From this population of solutions \mathbf{S} , the vec-
 274 tor of fitness $(f(S_1), f(S_2), \dots, f(S_D))$ is evaluated (Step 2). If a legal solution
 275 S_d ($d \in \llbracket 1, D \rrbracket$) sothat $f(S_d) = 0$ is found in the population, the algorithm
 276 stops. Otherwise a global loss term \mathcal{L} (scalar) is computed (Step 3). \mathcal{L} aggre-
 277 gates three terms: (i) $f(\mathbf{S})$ the global coloring fitness of the candidate solutions
 278 (see Section 3.5), (ii) a penalization term $\kappa(\mathbf{S})$ for shared wrong color group
 279 assignments in the population (see Section 3.6.1) and (iii) a bonus term $\varpi(\mathbf{S})$
 280 for shared correct color group assignments (see Section 3.6.2). Finally, the
 281 gradient of the loss \mathcal{L} with respect to the weight tensor \mathbf{W} is evaluated and
 282 then used to update the weights by first order gradient descent (Step 4). In
 283 the following subsections, each of these steps is described in detail.

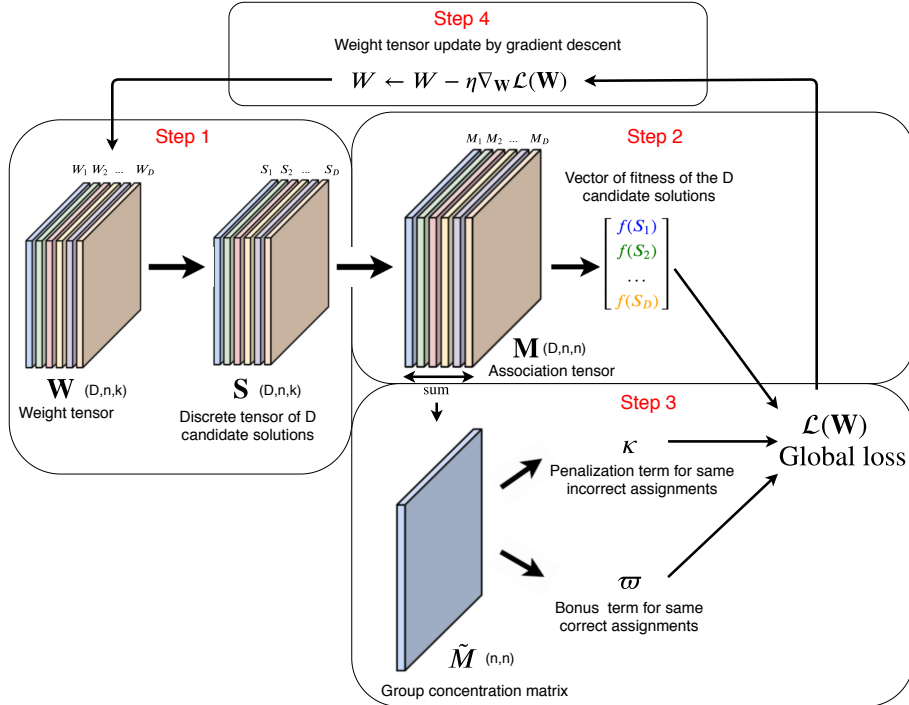


Fig. 1. General scheme of the TensCol algorithm

284 3.4 Step 1 - Vertex to color assignment

285 At each iteration of the TensCol algorithm, the current weight tensor \mathbf{W} is
 286 used to derive the associated tensor \mathbf{S} of candidate solutions as follows. For
 287 $(d, i, j) \in \llbracket 1, D \rrbracket \times \llbracket 1, n \rrbracket \times \llbracket 1, k \rrbracket$, $s_{d,i,j} = 1$ if $j = \operatorname{argmax}_{l \in \{1, \dots, k\}} w_{d,i,l}$ and $s_{d,i,j} = 0$
 288 if $j \neq \operatorname{argmax}_{l \in \{1, \dots, k\}} w_{d,i,l}$. This color group assignment for each vertex can be
 289 summarized as a single function $g(\mathbf{W}) = \text{one_hot}(\operatorname{argmax}(\mathbf{W}))$ from $\mathbb{R}^{D \times n \times k}$
 290 to $\{0, 1\}^{D \times n \times k}$, where argmax and one_hot operations are applied along the
 291 last axis of the tensor (color axis). Figure 2 shows an example with $D = 3$
 292 individuals in the population, $n = 5$ vertices and $k = 4$ colors.

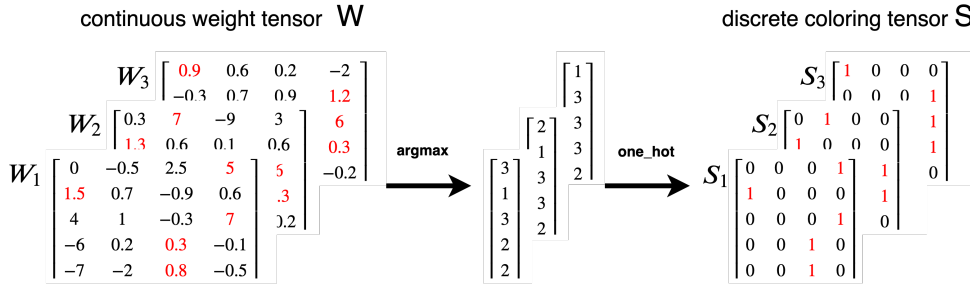


Fig. 2. Example of vertex to color assignment \mathbf{S} from a weight tensor \mathbf{W} , with $D = 3$, $n = 5$ and $k = 4$.

293 3.5 Step 2 - Fitness evaluation

294 For a graph $G = (V, E)$ with n vertices, let $A = \{a_{i,j}\}_{i,j=1 \dots n}$ be its adjacency
 295 matrix so that $\{v_i, v_j\} \in E$ if and only if $a_{i,j} = 1$. This symmetric matrix
 296 defines the coloring constraints to be respected by a legal coloring. The three-
 297 dimensional tensor \mathbf{A} is used to represent the D duplications of the adjacency
 298 matrix A .

299 Given \mathbf{S} the tensor of D candidate solutions, \mathbf{S}' denotes the transposed three-
 300 dimensional tensor obtained from \mathbf{S} by swapping its second and third axis and
 301 an *association tensor* \mathbf{M} is defined as $\mathbf{M} = \mathbf{S} \cdot \mathbf{S}'$, where \cdot is the dot product
 302 between two tensors (sum product over the last axis of \mathbf{S} and the second axis
 303 of \mathbf{S}').

304 For $(d, i, j) \in \llbracket 1, D \rrbracket \times \llbracket 1, n \rrbracket \times \llbracket 1, n \rrbracket$, each entry of \mathbf{M} is given by $m_{d,i,j} =$
 305 $\sum_{l=1}^k s_{d,i,l} s_{d,j,l}$. One notices that $m_{d,i,j} = 1$ if and only if the two vertices v_i
 306 and v_j in the solution S_d are assigned the same color (i.e. belong to the same
 307 color group). Interestingly enough this *association tensor* is independent by
 308 permutation of the columns in each candidate solution S_d (permutation of

the k colors)¹. Then, by performing the element-wise product between the tensors \mathbf{A} and \mathbf{M} , the global *conflict tensor* for the D solutions is obtained as $\mathbf{C} = \mathbf{A} \odot \mathbf{M}$, where \odot corresponds to the Hadamar product. For $(d, i, j) \in \llbracket 1, D \rrbracket \times \llbracket 1, n \rrbracket \times \llbracket 1, n \rrbracket$, each entry of \mathbf{C} is given by $c_{d,i,j} = a_{i,j}m_{d,i,j}$, and so $c_{d,i,j} = 1$ if and only if vertices v_i and v_j are *in conflict* in the candidate solution S_d , i.e., they are linked by an edge ($a_{i,j} = 1$) and are assigned to the same color group ($m_{d,i,j} = 1$). As $c_{d,i,j} = c_{d,j,i}$, the total number of conflicts or the *fitness* $f_{color}(S_d)$ of the candidate solution S_d is then given by

$$f_{color}(S_d) = \frac{1}{2} \sum_{i,j=1}^n c_{d,i,j}. \quad (1)$$

So the fitness vector containing D fitness values (conflicts) for the whole population of solutions \mathbf{S} is computed in parallel with a single tensor operation from \mathbf{C} as $(f_{color}(S_1), \dots, f_{color}(S_d)) = \frac{1}{2} \text{sum}(\mathbf{C}, (2, 3))$ where $\text{sum}(\cdot, (2, 3))$ is the summation operation along second and third axis. The *global coloring fitness* for the tensor \mathbf{S} of D candidate solutions can be evaluated as

$$f_{color}(\mathbf{S}) = \frac{1}{2} \text{sum}(\mathbf{C}). \quad (2)$$

For the classical GCP, any solution S_d satisfying $f_{color}(S_d) = 0$ is a legal coloring for the problem. As such, this global coloring fitness $f_{color}(\mathbf{S})$ is used as the global fitness function $f(\mathbf{S})$ to be minimized in the case of the GCP (see Section 3.1): $f(\mathbf{S}) = f_{color}(\mathbf{S})$.

For the ECP where the additional equity constraint is imposed, a supplementary equity fitness $f_{eq}(S_d)$ is introduced for each candidate solution S_d . Indeed, the equity constraint states that the number of vertices assigned to each of the k color groups must be equal to $c_1 = \lfloor \frac{n}{k} \rfloor$ or $c_2 = \lfloor \frac{n}{k} \rfloor + 1$ where $\lfloor \cdot \rfloor$ denotes the integer part of a positive real number and n is the number of vertices in G , with a particular case of $c_1 = c_2$ when n is divisible by k . To take into account the equity constraint, the additional *equity fitness* $f_{eq}(S_d)$ is defined as follows:

$$f_{eq}(S_d) = \sum_{l=1}^k \min(|\sum_{i=1}^n s_{d,i,l} - c_1|, |\sum_{i=1}^n s_{d,i,l} - c_2|). \quad (3)$$

¹ In the GCP and the ECP, two solutions S and S' , such that S' is equal to S up to a permutation of its k columns, are strictly equivalent in terms of fitness evaluation. It is very important to take into account this property in order to make relevant comparisons of the candidate solutions in the population.

334 It corresponds to the total number of surplus or deficit in terms of the num-
 335 ber of vertices in the color groups with respect to the admissible numbers of
 336 vertices c_1 and c_2 in each group. A legal solution S_d for the ECP must simul-
 337 taneously satisfy $f_{color}(S_d) = 0$ and $f_{eq}(S_d) = 0$. Let $f_{eq}(\mathbf{S}) = \sum_{d=1}^D f_{eq}(S_d)$ be
 338 the *global equity fitness* for the whole population \mathbf{S} of D candidate solutions.
 339 Then the global fitness function for the ECP (to be minimized) is given by
 340 $f(\mathbf{S}) = f_{color}(\mathbf{S}) + f_{eq}(\mathbf{S})$.

341 3.6 Step 3 - Computing global loss with penalization and bonus

342 Given a population \mathbf{S} of D solutions, the key idea is to introduce two depen-
 343 dency terms linking the D solutions for two considerations: discourage that the
 344 solutions repeat the same mistakes of creating conflicts for the same pairs of
 345 vertices (penalization) and encourage the solutions to consolidate the correct
 346 group assignments (bonus).

347 For this purpose, a summation of the association tensor \mathbf{M} (see Section 3.5)
 348 is performed along the first axis. The *group concentration matrix* \tilde{M} of size
 349 $n \times n$ is obtained:

$$\tilde{M} = \text{sum}(\mathbf{M}, 1), \quad (4)$$

350 For $(i, j) \in \llbracket 1, n \rrbracket \times \llbracket 1, n \rrbracket$, each entry of \tilde{M} is $\tilde{m}_{i,j} = \sum_{d=1}^D m_{d,i,j}$ which indicates
 351 the number of candidate solutions where vertices v_i and v_j are assigned to
 352 the same color group. The construction of this *group concentration matrix* is
 353 independent by permutation of the k colors (or k groups) of each candidate
 354 solution S_d .

355 3.6.1 Penalization term for shared wrong color assignments

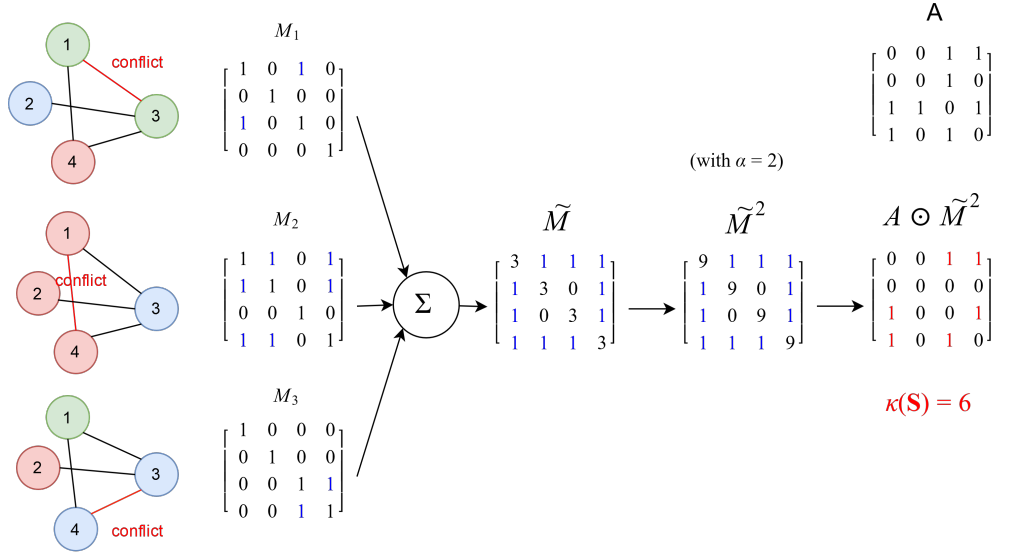
356 Using the *group concentration matrix* \tilde{M} above, the penalization term $\kappa(\mathbf{S}) =$
 357 $\text{sum}(A \odot \tilde{M}^{\circ \alpha})$ of the population \mathbf{S} is computed, where $\text{sum}(\cdot)$ corresponds
 358 to a sum of all matrix elements and \circ designates element-wise power tensor
 359 calculation.

$$\kappa(\mathbf{S}) = \sum_{i,j=1}^n a_{i,j} \tilde{m}_{i,j}^{\alpha}, \quad (5)$$

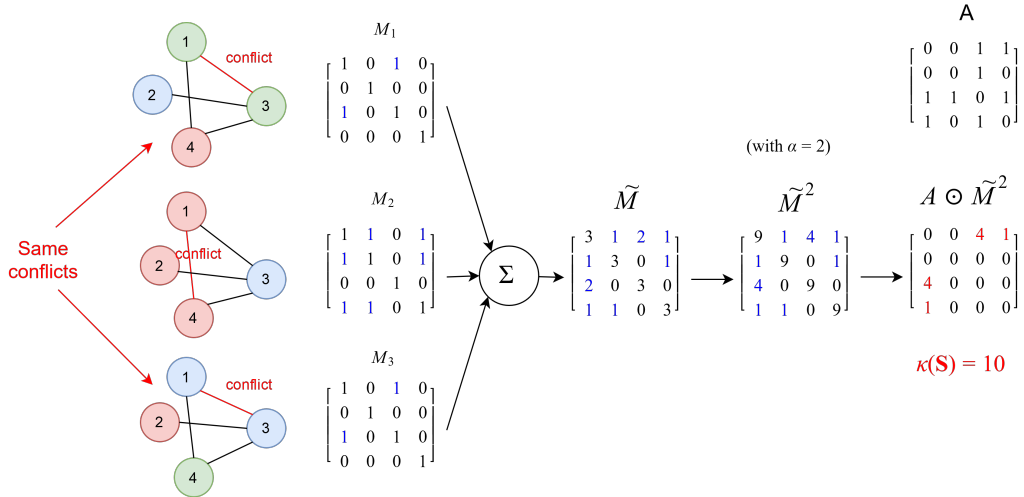
360 where α is a parameter greater than 1 in order to penalize the conflicts shared

by candidate solutions. By minimizing this term, the solutions are discouraged to make the same assignment mistakes for the same pair of vertices.

Figure 3 shows the computation of $\kappa(\mathbf{S})$ for a graph with $n = 4$ vertices, $k = 3$ colors and a population of 3 individuals. In both example 3a and 3b, there is one conflict in each candidate solution. However $\kappa(\mathbf{S}) = 6$ in example 3a as the conflicts are done for different edges, while $\kappa(\mathbf{S}) = 10$ (greater than 6) in example 3b because the first and the third candidate solutions make a conflict for the same edge $\{1, 3\}$ (even if different colors are used).



(a) $\kappa(\mathbf{S}) = 6$ for a population of 3 candidate solutions with different conflicts.



(b) $\kappa(\mathbf{S}) = 10 > 6$ for a population of 3 candidate solutions because two solutions share the same conflict on edge $\{1, 3\}$.

Fig. 3. Evaluation of $\kappa(\mathbf{S})$ for two populations of $D = 3$ candidate solutions with one conflict in each solution. There are $n = 4$ vertices in the graph that are colored with $k = 3$ colors. In this example α is set to 2.

369 3.6.2 Bonus term for shared correct color assignments

370 Then using the same idea the following bonus term $\varpi(\mathbf{S}) = \text{sum}(\bar{A} \odot \tilde{M}^{\circ\beta})$ is
 371 computed, where $\bar{A} = J - A$, with J the matrix of ones of size $n \times n$.

$$\varpi(\mathbf{S}) = \sum_{i,j=1}^n (1 - a_{i,j}) \tilde{m}_{i,j}^{\beta} \quad (6)$$

372 with β greater than 1.

373 By maximizing this bonus term, the D candidate solutions are encouraged to
 374 make the same correct color assignments for any pair of vertices.

375 3.6.3 Global loss function

376 The global loss function (to be minimized) aggregates the following three
 377 criteria: (i) the global coloring fitness $f_{color}(\mathbf{S})$ (equation (2)), (ii) the optional
 378 global equity fitness $f_{eq}(\mathbf{S})$ for the ECP (equation (3)), (iii) the penalization
 379 term for shared wrong color assignments $\kappa(\mathbf{S})$ (equation (5)) and (iv) the bonus
 380 term for shared correct color assignments $\varpi(\mathbf{S})$ (equation (6)), subtracted in
 381 order to maximize it.

$$\mathcal{L}(\mathbf{S})(t) = f_{color}(\mathbf{S}) + \nu t f_{eq}(\mathbf{S}) + \lambda t \kappa(\mathbf{S}) - \mu t \varpi(\mathbf{S}) \quad (7)$$

382 where $\nu \geq 0$ ($\nu = 0$ for the GCP since f_{eq} only concerns the ECP); $\lambda > 0$
 383 and $\mu > 0$ are the weighting factors for the penalization term and the bonus
 384 term, while $t \in \llbracket 0, maxIter \rrbracket$ is the iteration counter of the algorithm. The
 385 introduction of the time dependent parameter t aims to dynamically change
 386 the fitness landscape and increase the chance of the algorithm to get out of
 387 local minimum traps. Introducing the equity fitness progressively for the ECP
 388 improves the results as it leaves the possibility for the algorithm to find a legal
 389 coloring before having to consider the equity constraint too much.

390 3.7 Step 4 - Gradient descent

391 Gradient descent is a powerful optimization method that has been applied
 392 to various applications such as coefficient updates in linear regression and
 393 weight adjustments in neural networks [26], weighted nearest neighbors feature
 394 selection [8], and dimensionality reduction using similarity projections [38]. In
 395 the context of this work, since the set of candidate solutions \mathbf{S} derives from

396 \mathbf{W} (cf. Step 1 above), the problem is to optimize \mathbf{W} such that $\mathcal{L}(\mathbf{S})(t) =$
 397 $\mathcal{L}(g(\mathbf{W}))(t)$ is minimum with a first order gradient descent method. To make
 398 it easier, $\mathcal{L}(\mathbf{W})$ is written instead of $\mathcal{L}(g(\mathbf{W}))(t)$ hereafter.

399 Let $\nabla_{\mathbf{W}}\mathcal{L}(\mathbf{W})$ be the gradient tensor of $\mathcal{L}(\mathbf{W})$ with respect to \mathbf{W} of size
 400 $d \times n \times k$ whose element (d, i, j) is $\frac{\partial \mathcal{L}}{\partial w_{d,i,j}}$. Then the entries of the weight tensor
 401 \mathbf{W} can be updated at each iteration as

$$\mathbf{W} \leftarrow \mathbf{W} - \eta \nabla_{\mathbf{W}}\mathcal{L}(\mathbf{W}), \quad (8)$$

402 where $\eta > 0$ is a fix learning rate. This kind of first order optimization is
 403 classically used to learn neural networks (in stochastic version) and is known
 404 to be very efficient to learn models with a huge number of parameters.

405 However, in order to allow the method to escape local minima and forget
 406 old decisions that were made long ago and are no longer helpful, a weight
 407 smoothing inspired by the work [45] is applied. Every nb_{iter} iterations all the
 408 weights of \mathbf{W} are divided by a constant number $\rho \geq 1$, which can be achieved
 409 with a single tensor computation according to

$$\mathbf{W} \leftarrow \mathbf{W} / \rho. \quad (9)$$

410 This weight smoothing procedure can also be compared to the pheromone
 411 evaporation process used in Ant System (AS) [11] in the sense that the pheromone
 412 guides the ant search toward the most promising solutions, while a decay factor
 413 controls the rate at which historic information is lost.

414 3.8 Gradient computation with softmax approximation

415 To tackle this real-valued optimization problem by first order gradient descent
 416 over \mathbf{W} , $\nabla_{\mathbf{W}}\mathcal{L}(\mathbf{W})$ needs to be computed. By applying the chain rule [37], it
 417 gives for $d, i, j \in \llbracket 1, D \rrbracket \times \llbracket 1, n \rrbracket \times \llbracket 1, k \rrbracket$,

$$\frac{\partial \mathcal{L}}{\partial w_{d,i,j}} = \sum_{l=1}^k \frac{\partial \mathcal{L}}{\partial s_{d,i,l}} \times \frac{\partial s_{d,i,l}}{\partial w_{d,i,j}}. \quad (10)$$

418 3.8.1 Softmax approximation

419 Due to the use of the function *argmax* to build \mathbf{S} from \mathbf{W} , each partial term
 420 $\frac{\partial s_{d,i,l}}{\partial w_{d,i,j}}$ entering in equation (10) is equal to zero almost everywhere. Therefore,

421 the *softmax* function will be used as a continuous, differentiable approximation
 422 to *argmax*, with informative gradient.

423 \mathbf{S} can be approximated by a tensor $\hat{\mathbf{S}}$ of size $D \times n \times k$, where each $\hat{s}_{d,i,j}$ is
 424 computed with the elements of \mathbf{W} using the *softmax* function [7] as

$$\hat{s}_{d,i,j} = \frac{e^{w_{d,i,j}}}{\sum_{l=1}^k e^{w_{d,i,l}}}, \text{ for } d, i, j \in \llbracket 1, D \rrbracket \times \llbracket 1, n \rrbracket \times \llbracket 1, k \rrbracket. \quad (11)$$

425 Each entry $\hat{s}_{d,i,j} \in]0, 1[$ of the tensor $\hat{\mathbf{S}}$ denotes, for each candidate solution S_d ,
 426 a continuous indicator that the i -th vertex v_i selects the j -th color group g_j
 427 as its group. In the following this soft assignment is rewritten for each vertex
 428 with a single tensor equation as

$$\hat{S}(\mathbf{W}) = \text{softmax}(\mathbf{W}), \quad (12)$$

429 where the *softmax* function is applied along the last axis (color group axis)
 430 for each candidate solution and each vertex.

431 For d, i, j, l , $\frac{\partial s_{d,i,l}}{\partial w_{d,i,j}}$ is approximated by $\frac{\partial \hat{s}_{d,i,l}}{\partial w_{d,i,j}} = \hat{s}_{d,i,l}(\delta_{j,l} - \hat{s}_{d,i,j})$, with $\delta_{j,l}$ the
 432 Kronecker symbol equaling 1 if $j = l$ and 0 otherwise. Using this Straight-
 433 Through (ST) gradient estimator [4] of $\frac{\partial s_{d,i,l}}{\partial w_{d,i,j}}$ in equation (10), it gives for
 434 $d, i, j \in \llbracket 1, D \rrbracket \times \llbracket 1, n \rrbracket \times \llbracket 1, k \rrbracket$:

$$\frac{\partial \mathcal{L}}{\partial w_{d,i,j}} \approx \sum_{l=1}^k \frac{\partial \hat{s}_{d,i,l}}{\partial w_{d,i,j}} \times \frac{\partial \mathcal{L}}{\partial s_{d,i,l}} \quad (13)$$

$$= \sum_{l=1}^k \hat{s}_{d,i,l}(\delta_{j,l} - \hat{s}_{d,i,j}) \times \frac{\partial \mathcal{L}}{\partial s_{d,i,l}} \quad (14)$$

$$= \hat{s}_{d,i,j} \frac{\partial \mathcal{L}}{\partial s_{d,i,j}} - \hat{s}_{d,i,j} \sum_{l=1}^k \hat{s}_{d,i,l} \times \frac{\partial \mathcal{L}}{\partial s_{d,i,l}}. \quad (15)$$

435 In the proposed framework however, no sequential loop is used to calculate
 436 the gradient of each parameter. Instead a tensor product is simply computed
 437 to get the full gradient matrix. This operation can easily be parallellized on
 438 GPU devices. With tensor operations, the $D \times n \times k$ equations (15) for $d, i, j \in$
 439 $\llbracket 1, D \rrbracket \times \llbracket 1, n \rrbracket \times \llbracket 1, k \rrbracket$ become then a single equation:

$$\nabla_{\mathbf{W}} \mathcal{L} = \hat{\mathbf{S}} \odot (\nabla_{\mathbf{S}} \mathcal{L} - (\hat{\mathbf{S}} \odot \nabla_{\mathbf{S}} \mathcal{L}) \cdot J), \quad (16)$$

440 where $\nabla_{\mathbf{S}} \mathcal{L} = \{\frac{\partial \mathcal{L}}{\partial s_{d,i,j}}\}_{d,i,j}$ is the gradient matrix of size $D \times n \times k$ of \mathcal{L} with

respect to \mathbf{S} , J is a matrix of 1's of size $k \times k$, \odot is the Hadamard product
(element-wise product) and \cdot is the dot product between two tensors.

3.8.2 Gradient of \mathcal{L} with respect to \mathbf{S}

In order to compute $\nabla_{\mathbf{W}}\mathcal{L}(\mathbf{W})$ with equation (16), it remains to compute
 $\nabla_{\mathbf{S}}\mathcal{L}$. According to equation (7), it gives

$$\begin{aligned}\mathcal{L}(\mathbf{S})(t) &= f_{color}(\mathbf{S}) + \nu t f_{eq}(\mathbf{S}) + \lambda t \kappa(\mathbf{S}) - \mu t \varpi(\mathbf{S}) \\ &= \frac{1}{2} \text{sum}(\mathbf{A} \odot (\mathbf{S} \cdot \mathbf{S}')) + \nu t f_{eq}(\mathbf{S}) + \lambda t \text{sum}(A \odot \tilde{M}^{\circ\alpha}) \\ &\quad - \mu t \text{sum}(\bar{A} \odot \tilde{M}^{\circ\beta}).\end{aligned}$$

At iteration t , the gradient of this loss with respect to the tensor \mathbf{S} of D
solutions is then given by²

$$\nabla_{\mathbf{S}}\mathcal{L}(t) = A \cdot \mathbf{S} + \nu t \nabla_{\mathbf{S}} f_{eq}(\mathbf{S}) + 2\alpha \lambda t (A \odot \tilde{M}^{\circ(\alpha-1)}) \cdot \mathbf{S} - 2\beta \mu t (\bar{A} \odot \tilde{M}^{\circ(\beta-1)}) \cdot \mathbf{S}, \quad (17)$$

where $\nabla_{\mathbf{S}} f_{eq}(\mathbf{S})$ is the gradient of the additional global equity fitness. For
 $d, i, j \in \llbracket 1, D \rrbracket \times \llbracket 1, n \rrbracket \times \llbracket 1, k \rrbracket$, each entry (d, i, j) of $\nabla_{\mathbf{S}} f_{eq}(\mathbf{S})$ is equal to

$$\frac{\partial f_{eq}(\mathbf{S})}{\partial s_{d,i,j}} = \begin{cases} 0 & \text{if } \#V_{d,j} = c_1 \text{ or } \#V_{d,j} = c_2 \\ +1 & \text{if } \#V_{d,j} > c_2 \\ -1 & \text{if } \#V_{d,j} < c_1 \end{cases} \quad (18)$$

with $\#V_{d,j} = \sum_{i=1}^n s_{d,i,j}$ the total number of vertices receiving color j for the
candidate solution d .

² Let us note that the first term $A \cdot S$ in equation (17), the gradient of $f_{color}(\mathbf{S})$, corresponds to the γ -matrix used in an efficient implementation proposed in [15] of the popular TabuCol algorithm for the GCP [22].

3.9 General TensCol algorithm

The general TensCol algorithm involving the above-mentioned four steps is summarized in Algorithm 1.

The algorithm iterates the four composing steps (Sections 3.4-3.7) until one of the following stopping conditions is reached: 1) the global fitness of one of the D candidate solutions in \mathbf{S} reaches 0 (i.e., a legal k -coloring is found); 2) the number of iterations reaches the allowed limit $maxIter$. One can notice from Algorithm 1 that it is not necessary to evaluate the penalization term $\kappa(\mathbf{S})$ and bonus terms $\varpi(\mathbf{S})$. It saves computational and memory resources to compute only their gradients with respect to \mathbf{S} .

The only stochastic part in TensCol concerns the initialization of the tensor \mathbf{W} whose weights are drawn randomly according to a normal law. This random initialization has an impact on the search. Therefore for practical performance evaluation, the algorithm will be run a lot of times with different random seeds r to initialize the pseudo-random generator of the normal law.

The time complexity of each step of the algorithm is given in Table 1. The most costly operation is in $O(Dn^2k)$. Therefore the main factor influencing the execution time of the algorithm is n , the size of the graph. This complexity is alleviated in practice thanks to two factors. First, the tensor operations of the algorithm greatly benefit from our implementation with the Pytorch library specially designed for the parallel calculation of tensors on GPU devices. Second, unlike local search based coloring algorithms where each iteration only changes the color of one single vertex in a candidate solution, each iteration of the TensCol algorithm may simultaneously change the colors of many vertices, because each iteration may update the $n * k$ weights of the solution (see the example in the next section). Moreover, our experiments showed that this is quite useful to deal with large graphs, helping to find several record-breaking results for the ECP, as shown in Section 5.4.

4 First experimental analysis

In this section, an illustrative toy example is first presented for the GCP (subsection 4.1) to give intuitive insights on the gradient descent learning. In Subsection 4.2, a sensitivity analysis of the main parameters λ and μ is presented in order to show the importance of the penalization and bonus terms in the global loss function used by the algorithm. Then in subsection 4.3, the fitness evolution of the algorithm during the search is shown.

Algorithm 1 TensCol for graph coloring problems

Input: graph G with adjacency matrix A , available colors $\{1, 2, \dots, k\}$, random seed r , and number of maximum allowed iterations $maxIter$;

Output: a legal k -coloring G if it is found;

$\mathbf{W} \leftarrow \mathbf{W}_0$ /* Weight tensor initialization: $w_{i,j,d}^0 \sim \mathcal{N}(0, \sigma_0)$ with random seed r */

$t \leftarrow 0$

repeat

Step 1) Vertex to color assignment

 i) $\mathbf{S} = \text{one_hot}(\text{argmax}(\mathbf{W}))$

Step 2) Fitness evaluation (forward phase)

 i) $\mathbf{M} = \mathbf{S} \cdot \mathbf{S}'$

 ii) $\mathbf{C} = \mathbf{A} \odot \mathbf{M}$

 iii) Compute the vector of fitness $(f(S_1), \dots, f(S_D))$

Step 3) Group concentration matrix, penalization and bonus terms evaluation

 i) $\tilde{M} = \text{sum}(\mathbf{M}, 1)$

 ii) Compute $\nabla_{\mathbf{S}} \mathcal{L}(t) = A \cdot \mathbf{S} + \nu t \nabla_{\mathbf{S}} f_{eq}(\mathbf{S}) + 2\alpha \lambda t (A \odot \tilde{M}^{\circ(\alpha-1)}) \cdot \mathbf{S} - 2\beta \mu t (\bar{A} \odot \tilde{M}^{\circ(\beta-1)}) \cdot \mathbf{S}$

Step 4) Weight update by gradient descent

 i) Compute $\hat{\mathbf{S}} = \text{softmax}(\mathbf{W})$;

 ii) $\nabla_{\mathbf{W}} \mathcal{L} = \hat{\mathbf{S}} \odot (\nabla_{\mathbf{S}} \mathcal{L} - (\hat{\mathbf{S}} \odot \nabla_{\mathbf{S}} \mathcal{L}) \cdot J)$

 iii) $\mathbf{W} \leftarrow \mathbf{W} - \eta \nabla_{\mathbf{W}} \mathcal{L}$;

 iv) Every nb_{iter} do $\mathbf{W} \leftarrow \mathbf{W} / \rho$;

$t \leftarrow t + 1$

until $\min_d f(S_d) = 0$ or $t = maxIter$

if $\min_d f(S_d) = 0$ **then**

return S_{d^*} with $d^* = \underset{d}{\operatorname{argmin}} f(S_d)$

end if

487 4.1 Toy example for the graph coloring problem

488 A simplified implementation of TensCol is used for the GCP, where only one
489 candidate solution is evaluated ($D = 1$). It is applied to an easy graph named
490 myciel4.col of the COLOR02 benchmark with 21 vertices and known chromatic
491 number of 5. Figure 4 displays the last 3 iterations (over 8) of TensCol to
492 color myciel4.col with 5 colors and random seed $r = 0$. The parameters used

Table 1

Time complexity of each step of the algorithm.

Step	Type of operation	Time complexity
Step 1 - i)	Finding the color with max weight value for each vertex	$O(Dnk)$
Step 2 - i)	Tensor dot product between two tensors of size (D, n, k) and (D, k, n)	$O(Dn^2k)$
Step 2 - ii)	Element wise multiplication between two tensors of size (D, n, n)	$O(Dn^2)$
Step 2 - iii)	Fitness vector computation	$O(Dn^2)$
Step 3 - i)	Sum along first axis of a tensor of size (D, n, n)	$O(Dn^2)$
Step 3 - ii)	Computation of the gradient of the loss with respect to S	$O(Dn^2k)$
Step 4 - i)	Tensor softmax operation	$O(Dnk)$
Step 4 - ii)	Computation of the gradient of the loss with respect to W	$O(Dnk)$
Step 4 - iii)	Tensor subtraction	$O(Dnk)$
Step 4 - iii)	Tensor division	$O(Dnk)$

in TensCol are $\lambda = 0$, $\mu = 0$, $\eta = 0.001$, $nb_{iter} = 5$ and $\rho = 200$. The number written on each vertex indicates the gradient of the fitness with respect to the selected color for this vertex. It corresponds to the total number of conflicts, i.e., adjacent vertices receiving the same color. Red edges correspond to conflicting edges. Blue circles highlight the vertices that change their color from one iteration to another. As one can see on this figure, TensCol tends to change the color of the vertices with the highest gradient values. One can also notice that TensCol can change the color of more than one vertex at each iteration as the update is done on the full candidate solution matrix S at each iteration. A legal coloring solution S^* is shown in Figure 4 (d) with $f(S^*) = 0$.

4.2 Sensitivity analysis

This section investigates the usefulness of the penalization term for shared incorrect group assignments $\kappa(\mathbf{S})$ and the bonus term for shared correct group assignments $\varpi(\mathbf{S})$, which are two important parts of the global loss function (equation 7) with the two weighting factors λ and μ . For this study, a population of $D = 200$ candidate solutions launched in parallel is adopted.

The two dimensional heat map presented in Figure 5 shows the average best global fitness obtained by TensCol on the DSJC250.5.col instance with 250 vertices from the second competition organized by the Center for Discrete Mathematics and Theoretical Computer Science (DIMACS). This average fitness is computed from 20 different runs, each run performing 200,000 iterations with a new random initialization and new values for λ and μ from the range of 0 to 1.

When $\lambda = 0$ and $\mu = 0$, meaning that there are no interactions between the D candidate solutions, TensCol fails to obtain a good solution in the allotted time. The parameter that plays the most crucial role is λ which is used to

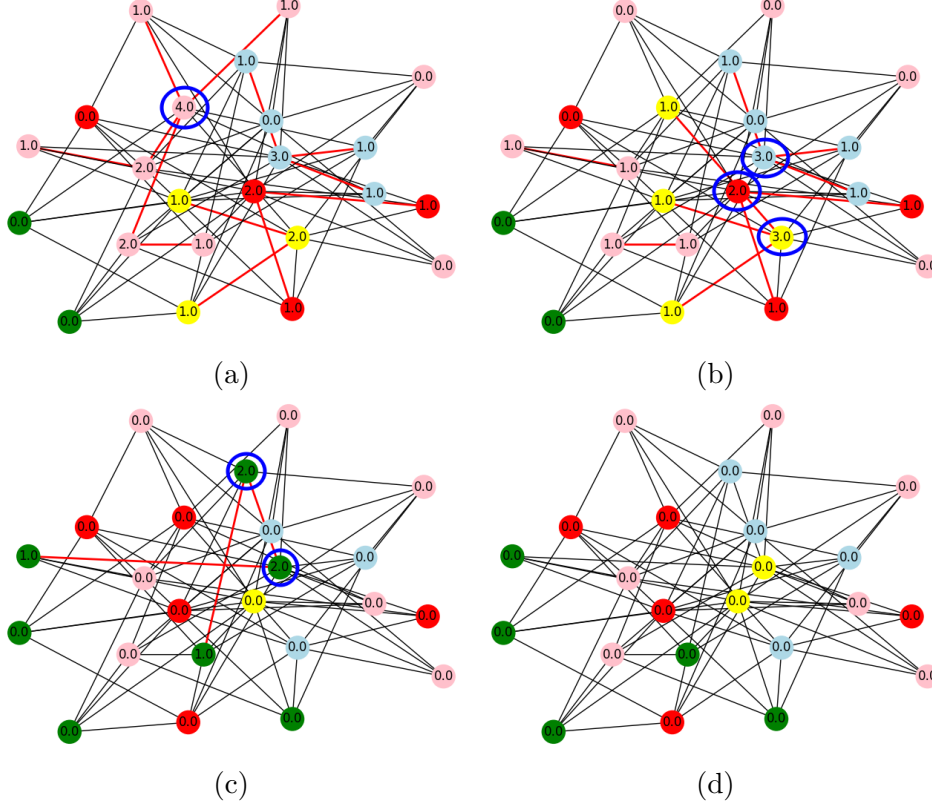


Fig. 4. **Last three iterations of TensCol** to color the graph myciel4.col with 5 colors (optimal value). The number on each vertex indicates the gradient of the global fitness score with respect to the selected color for this vertex. Red edges corresponds to conflicting edges. Blue circles highlight the vertices changing their color from one iteration to another. Several vertices can change their colors during the same iteration. Better seen in color.

penalize shared incorrect group assignments of the D solutions. Best results are obtained for $\lambda \in [1e-05, 1e-04]$. Furthermore the parameter μ used with the bonus term to encourage shared correct pairwise assignments, also helps to improve the results when it takes values between $1e-06$ and $1e-05$. However, its impact is less important than λ . If μ is set too high, the results deteriorate as the D candidate solutions are not diverse anymore. Best results with an average fitness equal to 0.0 (corresponding to a success rate of 100% on the 20 different runs) are obtained for the pairs $(\lambda = 10^{-5}, \mu = 10^{-6})$ and $(\lambda = 10^{-4}, \mu = 10^{-5})$. The first pair of values $(\lambda = 10^{-5}, \mu = 10^{-6})$ will be kept in the comparative benchmark evaluation presented in this work.

4.3 Evolution of the loss function

To illustrate how the objective converges during the learning and search process, the fitness evolution is studied when applying TensCol to color the ran-

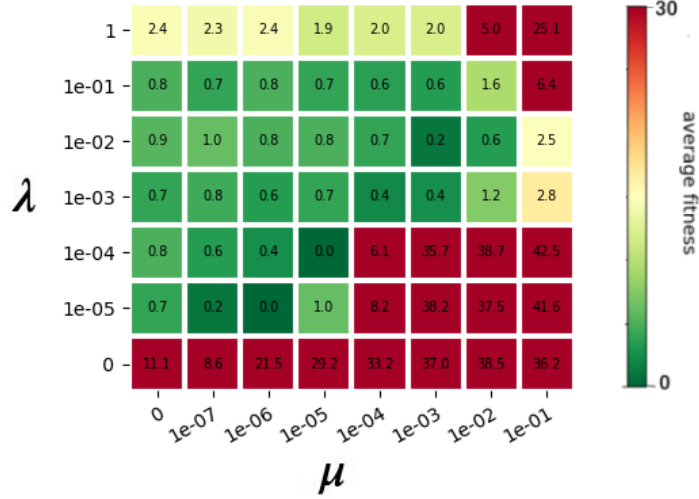


Fig. 5. Sensitivity analysis of λ (weighting factor for the penalization term) and μ (weighting factor for the bonus term) over the average global fitness of the graph DSJC250.5.col for the GCP. The average fitness is computed from the best global fitness values of 20 different runs, each run performing 200 000 iterations with a new random initialization. Best results are in green.

dom graph R250.5.col (250 vertices) with 65 colors (chromatic number). The algorithm is launched with the parameters $D = 200$, $\rho = 10$, $nb_{iter} = 5$, $\alpha = 2.5$, $\lambda = 10^{-5}$, $\beta = 1.2$, $\mu = 10^{-6}$ (for the GCP) and $\nu = 10^{-5}$ (for the ECP).

TensCol reaches a legal coloring (for the GCP) with 17,000 iterations on average (this corresponds to 3.4 million fitness evaluations since 200 candidate solutions are evaluated at the same time). It takes 33 seconds on average to find the solution on a Nvidia RTX2080Ti GPU card with a success rate of 100%.

Figure 6 shows that for the GCP, the fitness improves very quickly at the beginning to reach a score of around 15 conflicts and gradually decreases until a legal solution is found. For the ECP, Figure 7 indicates oscillations of the equity fitness (in red) as the algorithm quickly moves between equitable and non-equitable colorings during the search before reaching a feasible coloring. Small oscillation peaks appear due to the process of resetting the weights to avoid local optima (cf. Step 4-iv in Algorithm 1).

Finally, the objective convergence profile observed on the graph R250.5.col represents a typical search behavior of the algorithm.

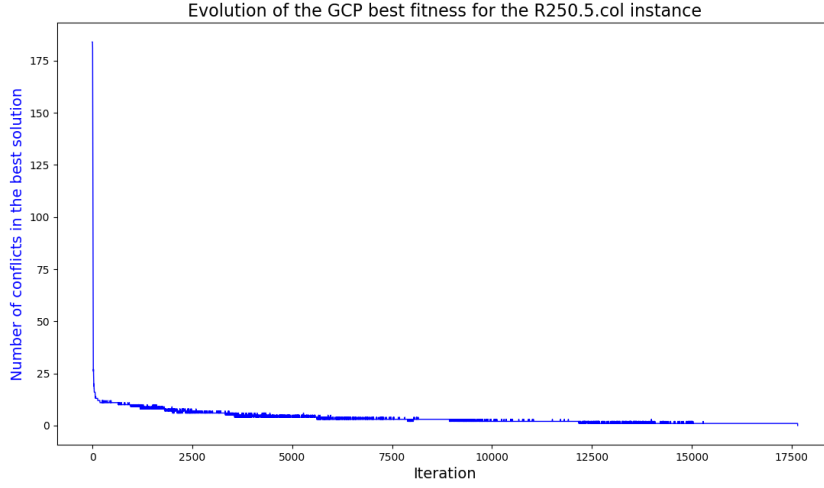


Fig. 6. Evolution of the number of conflicts obtained by the best solution among the 200 candidate solutions during the search for a legal coloring with 65 colors for the random graph R250.5.col.

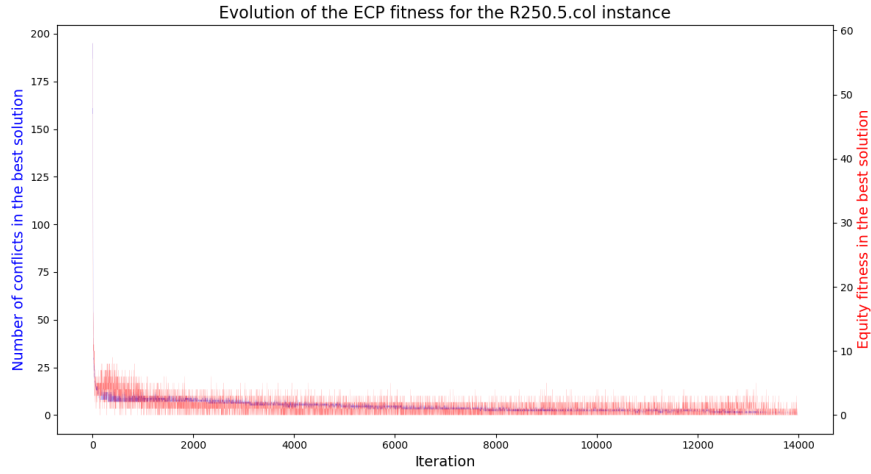


Fig. 7. Evolution of the number of conflicts (in blue) and the equity fitness (in red) obtained by the best solution among the 200 candidate solutions during the search for a feasible coloring with 65 colors for the random graph R250.5.col.

5 Computational results

This section is dedicated to a computational assessment of the TensCol algorithm for solving the two target graph coloring problems (i.e., GCP and ECP). The benchmark instances are first presented (subsection 5.1), followed by the experimental setting of TensCol for both problems (subsection 5.2). Then, the computational results obtained on the GCP are shown in subsection 5.3, and the results on the ECP are presented in subsection 5.4. An analysis and discus-

sions of the results obtained on different graph structures are then proposed in subsection 5.5.

5.1 *Benchmark instances and comparison criterion*

For the GCP, the TensCol algorithm is evaluated on the 36 most difficult benchmark instances from the second DIMACS competition³ that were used to test graph coloring algorithms in recent studies including the two individual memetic algorithm [35] and the probabilistic learning based algorithm [44]. For the ECP, the same set of 73 benchmark instances used in [39,42] from the second DIMACS and COLOR02 competitions⁴ is adopted.

Following the common practice to report comparative results in the coloring literature, the assessment focuses on the best solution found by each algorithm corresponding to the smallest number k of colors needed to reach a legal coloring for a graph. It is worth mentioning that for the GCP, no single algorithm in the literature including the most recent algorithms can attain the best-known results for all 36 difficult DIMACS instances. Indeed, even the best performing algorithms miss at least two best-known results. This is understandable given that these instances have been studied for a long time (over some 30 years) and some best-known results have been achieved only by very few algorithms under specific and relaxed conditions (e.g., large run time from several days to one month). Moreover, one notices that for these benchmark graphs, even finding a legal k -coloring is a difficult task if k is set to a value slightly above the chromatic number or the current best-known result. In other words, it is extremely difficult and unlikely to find improved solutions for these graphs. As such, an algorithm able to attain (or draw near to) the best-known results for a majority of the benchmark instances can be qualified promising with respect to the current state-of-the-art on graph coloring. Most of the above comments remain valid for the ECP.

Given these comments, one understands that for graph coloring problems (and in general for hard combinatorial optimization), computation time is not the main concern for performance assessment. This is also because the state-of-the-art algorithms (implemented with different programming languages) often report different results for some graphs, which were obtained on various computing platforms with specific stopping conditions (e.g., maximum allowed generations or iterations, maximum allowed fitness evaluations, a cutoff time limit etc). As a result, the timing information, when it is shown, is provided for indicative purposes only.

³ Publicly available at <ftp://dimacs.rutgers.edu/pub/challenge/graph/benchmarks/color/>

⁴ Publicly available at <https://mat.gsia.cmu.edu/COLOR02/>

594 The TensCol algorithm was implemented in Python 3.5 with Pytorch 1.1 li-
 595 brary for tensor calculation with CUDA 10.0⁵. It is specifically designed to
 596 run on GPU devices. In this work a Nvidia RTX 2080Ti graphic card with 12
 597 GB memory was used. A Nvidia Tesla P100 with 16 GB memory was used
 598 only for the two very large graphs (C2000.5.col and C2000.9.col instances).

599 For a small graph such as r250.5.col colored with $k = 65$ colors for an equi-
 600 table coloring, when TensCol is launched with $D = 200$ candidate solutions
 601 in parallel, $200 * 250 * 65 = 3.2$ millions weights $w_{d,i,j}$ are updated at each
 602 iteration. On a Nvidia RTX 2080Ti graphic card, it takes 0.002 seconds per
 603 iteration (for 200 candidate solutions evaluated). For a large graph such as
 604 C2000.9.col colored with $k = 431$ colors for an equitable coloring, there are
 605 $200 * 2000 * 431 = 172$ millions weights updated at each iteration. On a Nvidia
 606 Tesla P100, it takes 0.37 seconds per iteration.

607 To identify appropriate values for TensCol’s parameters, a grid search is ap-
 608 plied on a set of representative instances (DSJC250.5.col, DSJC250.9.col,
 609 DSJC500.5.col, DSJC500.9.col, DSJR500.1c.col, DSJR500.5.col, R250.5.col,
 610 R1000.1.col). For the grid search, each parameter is set within a reason-
 611 able range ($\lambda \in \{10^{-4}, 10^{-5}, 10^{-6}\}$, $\mu \in \{10^{-5}, 10^{-6}, 10^{-7}\}$ (for the GCP),
 612 $\nu \in \{10^{-4}, 10^{-5}, 10^{-6}\}$ (for the ECP), $\alpha \in \{1.5, 2, 2.5\}$, $nb_{iter} \in \{5, 10, 100\}$,
 613 $\beta \in \{1.2, 1.5, 2\}$ and $\rho \in \{1, 2, 10, 100, 200\}$) while keeping the other param-
 614 eter values with their default values $D = 200$, $\sigma_0 = 0.01$ and $\eta = 0.001$. An
 615 early stopping iteration criterion of 10^5 iterations is used to quickly stop the
 616 algorithm if the score no longer improves. The grid search allowed us to de-
 617 termine a best baseline parameter setting, given in Table 2, for the GCP and
 618 the ECP, which are kept for all instances, except for the smoothing parameter
 619 ρ which is very sensitive to the graph structure. The value of this parameter
 620 is thus chosen among 5 different values for each graph. For very difficult ran-
 621 dom graphs such as DSJC500.5.col and DSJC1000.5.col, the values $\rho = 100$ or
 622 $\rho = 200$ are used in order to frequently smooth the learned weight tensor \mathbf{W}
 623 according to equation (9). However, for geometric graphs such as R1000.1.col
 624 or instances based on register allocation such as fpsol2.i.1.col or mulsol.i.1.col,
 625 the value $\rho = 1$ is used meaning that no smooth process is applied during the
 626 search.

627 For some particular instances, it is necessary to deviate from this baseline pa-
 628 rameter setting in order to reach the state-of-the-art results. For the random
 629 DSJC graphs with a high density (DSJC125.9.col, DSJC250.9.col, DSJC500.9.col
 630 and DSJC1000.9.col), the value $\alpha = 1.5$ is adopted instead of $\alpha = 2.5$ in or-

⁵ The source code of our algorithm is available at <https://github.com/GoudetOlivier/TensCol>.

Table 2

Parameter setting in TensCol for the GCP and the ECP

Parameter	Description	Value for the GCP	Value for the ECP
D	number of candidate solutions	200	200
σ_0	standard deviation of initial parameters	0.01	0.01
η	learning rate	0.001	0.001
nb_{iter}	smoothing procedures period	5	5
ρ	smoothing parameter	{1,2,10,100,200}	{1,2,10,100,200}
α	exponent for the penalization term	2.5	2.5
λ	weighting factor for the penalization term	10^{-5}	10^{-5}
β	exponent for the bonus term	1.2	1.2
μ	weighting factor for the bonus term	10^{-6}	0.0
ν	weighting factor for the equity constraint	0.0	10^{-5}

der to prevent the penalization term $\kappa(S)$ from becoming too important (cf. equation (5)). On the contrary, for the random DSJC graphs with a low density (DSJC125.1.col, DSJC250.1.col, DSJC500.1.col and DSJC1000.1.col), the parameter μ is set to 10^{-7} for the GCP instead of 10^{-6} to avoid that the bonus term $\varpi(S)$ (cf. equation (6)) becomes too preponderant in the global loss evaluation. Specific fine tuning of the parameters are also done in the best performing methods such as HEAD [35] and QA [41].

For all the tested instances, the stopping criterion used is a maximum allowed number of iterations of 2×10^6 , which corresponds to a maximum of 4×10^8 evaluations of candidate solutions (as there are 200 solutions evaluated at each iteration). For the experiments, each instance was solved 10 times independently (with 10 different random seeds) following the common practice in the literature for graph coloring.

5.3 Computational results on graph coloring benchmark instances

This section is dedicated to an extensive experimental evaluation of TensCol on the GCP. A comparison of TensCol with 5 best-performing coloring algorithms is proposed (see Section 2.1 for a presentation of these algorithms):

- the two-phase evolutionary algorithm (MMT, 2008) [30] ran on a 2.4 GHz Pentium processor with a cut-off time of 1.6 or 11.1 hours;
- the distributed evolutionary quantum annealing algorithm (QA, 2011) [41] ran on a 3.0 GHz Intel processor with 12 cores with a cut-off time of 5 hours;
- the population-based memetic algorithm (MA, 2010) ran on a 3.4 GHz processor with a cut-off time of 5 hours;
- the latest hybrid evolutionary algorithm in Duet (HEAD, 2018) [35] ran in parallel on a 4 cores 3.1 GHz Intel Xeon processor with a cut-off time of at least 3 hours;

657 • the probability learning based local search (PLSCOL, 2018) [44] ran on an
658 Intel Xeon E5-2760 2.8 GHz processor with a cut-off of 5 hours.

659 To the best of our knowledge, these reference algorithms represent the state-
660 of-the-art for the GCP, which cover the current best-known results in the
661 literature for the difficult graphs used in this work.

662 Detailed results of TensCol and the reference algorithms on the 36 DIMACS
663 graphs are reported in Tables 4 and 5 in the Appendix. Columns 1 and 2
664 indicate the name and the number of vertices in each instance. Column 3
665 shows the chromatic number $\chi(G)$ (if known)⁶, while column 4 (k^*) gives the
666 best-known results (best upper bound of $\chi(G)$) ever reported by an algorithm.
667 Columns 5 to 19 show the best results (k_{best}) of the reference algorithms with
668 their success rate and computation time (in seconds). The remaining columns
669 report the results of our TensCol algorithm: the best result (k_{best}), the success
670 runs (SR) over 10 runs during which TensCol attained its best result, and the
671 average computation time (t(s)) for a successful run. A '-' symbol indicates
672 that the corresponding result is not available. As discussed in Section 5.1,
673 computation times were provided for indicative purposes.

674 As one can observe from Tables 4 and 5, TensCol always finds the best-known
675 coloring for the instances with less than 200 vertices such as DSJC125.1.col or
676 R125.1. On medium graphs with up to 500 vertices such as DSJC250.5.col or
677 DSJC500.5.col, TensCol is competitive compared to all reference algorithms. For
678 the two large random DSJC1000.5.col and DSJC1000.9.col instances, TensCol
679 performs better than PLSCOL and MMT, but worse than the two best-
680 performing memetic algorithms MA and HEAD. For the family of flat graphs,
681 MA and HEAD perform the best. But these graphs (especially flat300_28.0
682 and flat1000_76.0 graph) remain difficult for all the algorithms.

683 TensCol performs very well on the whole family of 7 geometric graphs by
684 attaining all the best-known results and in particular reports a 234-coloring
685 on the very difficult R1000.5.col graph. This is a remarkable result because
686 this 234-coloring, which was first reported in 2008 by the highly sophisti-
687 cated MMT algorithm [30], has never been reproduced by another algorithm
688 since that date. TensCol also obtains an excellent 98-coloring for the large
689 latin_square_10 graph, which remains difficult for the reference algorithms ex-
690 cept QA which reported the same result as TensCol.

691 Finally, given the particularity of the GCP benchmark instances as discussed
692 in Section 5.1, it is not suitable to apply statistical tests.

⁶ For some instances such as flat1000_76.0 the chromatic number is known by con-
struction of the graph (and equal to 76 in this case), but no heuristic has yet found
a legal coloring with the chromatic number.

694 This section reports a comparison of TensCol with 5 most recent state-of-the-
695 art algorithms in the literature for the ECP (more details of these algorithms
696 are given in Section 2.2):

- 697 • the tabu search algorithm (TabuEqCol, 2014) [12];
- 698 • the backtracking based iterated tabu search (BITS, 2015) [25];
- 699 • the feasible and infeasible search algorithm (FISA, 2017) [39];
- 700 • the hybrid tabu search (HTS, 2018) [42];
- 701 • the memetic algorithm (MAECP, 2020) [40].

702 The results of TabuEqCol were obtained on a computer with an Intel i5
703 CPU750 2.67GHz processor under a cutoff limit of 1h, while the four other
704 reference algorithms were run on an Intel Xeon E5440 2.83 GHz processor (or
705 a comparable processor) with a cutoff time of 2.7h for the instances with upto
706 500 vertices and 11 hours for larger instances. Given that TabuEqCol is the
707 oldest algorithm among the reference algorithms, it is no surprise that it is
708 dominated by the other algorithms. TabuEqCol is included in this study as it
709 is a baseline reference for the ECP.

710 Tables 6 - 9 show the best results of the six compared algorithms in terms of the
711 smallest number of colors used to color each graph with the equity constraint
712 for the DIMACS and COLOR02 instances. Column 3 displays the overall best-
713 known result k^* of the ECP ever reported in the literature. The next fifteen
714 columns report the best results by the reference algorithms (TabuEqCol, BITS,
715 FISA, HTS and MAECP) with their success rate and computation time (in
716 seconds). The last three columns show the results of our Tensol algorithm. A
717 '-' symbol indicates that the corresponding result is not available. Like for the
718 GCP, the assessment focuses on the quality criterion and timing information
719 is provided for indicative purposes only.

720 From the results of Tables 6 - 9, one can observe that in terms of attaining
721 the best-known results, TensCol is the second best performing algorithm after
722 the most recent MAECP algorithm (12 best-known results missed by TensCol
723 against 8 best-known results missed by MAECP). In particular, for the graphs
724 with up to 500 vertices, TensCol obtains comparable results with the state-
725 of-the-art algorithms, except for DSJC500.9.col, le450_15a.col, le450_15b.col,
726 le450_25c.col and le450_25d.col where TensCol performs worse than some ref-
727 erence algorithms, but it is better on the DSJC500.5.col instance than most
728 competitors. For the wapXXa.col instances, the results obtained by TensCol
729 are not so good as the other algorithms.

730 On the contrary, TensCol excels on large graphs between 900 and 2000 ver-
731 tices. Remarkably, it established 8 new best-known records (new upper bounds

summarized in Table 3) by finding legal and equitable colorings with fewer colors compared to the current best-known k^* values. As one can observe in Table 3, TensCol significantly improves the best-known upper bound for three large graphs with 37 colors less for C2000.9.col, 9 colors less for C2000.5.col and 8 colors less for R1000.5.col, while the improvement for the 6 other cases goes from -1 to -3 colors. These new solutions are available at <https://github.com/GoudetOlivier/TensCol>.

Table 3

New record coloring results found by TensCol for 8 large benchmark graphs. Some improvements are very important with a gain of 8, 9 and 37 colors.

Instance	$ V $	previous best-known k^*	new best-known k^*	Improvement
DSJR500.5.col	500	124	122	-2
DSJC1000.5.col	1000	95	92	-3
R1000.5.col	1000	247	239	-8
flat1000.60.0.col	1000	93	92	-1
flat1000.76.0.col	1000	93	91	-2
latin_square_10.col	900	103	102	-1
C2000.5.col	2000	183	172	-9
C2000.9.col	2000	468	431	-37

5.5 Analysis of the results and discussions

This section discusses the reasons behind the results presented in the comparative study of the last two subsections.

5.5.1 Analysis of the graph coloring results

One can notice in Tables 4 and 5 that compared to most reference algorithms, TensCol competes favorably on the *geometric* graphs such as the large R1000.5.col graph by finding 234-colorings. Meanwhile, compared to some reference algorithms, TensCol is less competitive on some *random* graphs such as DSJC500.5.col and DSJC1000.5.col.

To better understand these results, one can look at the structure of the solutions obtained with the TensCol algorithm for the random graphs DSJC250.5.col ($k = 28$) and DSJC1000.5.col ($k = 84$), and for the geometric graphs R250.5.col ($k = 65$) and R1000.5.col ($k = 234$). All these graphs have an edge density of 0.5. However the distributions of the sizes of the color groups in the solutions for these two types of graphs are very different as shown in Figure 8. For the random graphs DSJC250.5.col and DSJC1000.5.col, there are important variations in color group sizes with many (12 to 15) shared vertices, while the color groups in the solutions of the geometric graphs are more homogeneous,

757 mainly with small color groups of size 4 or 5⁷.

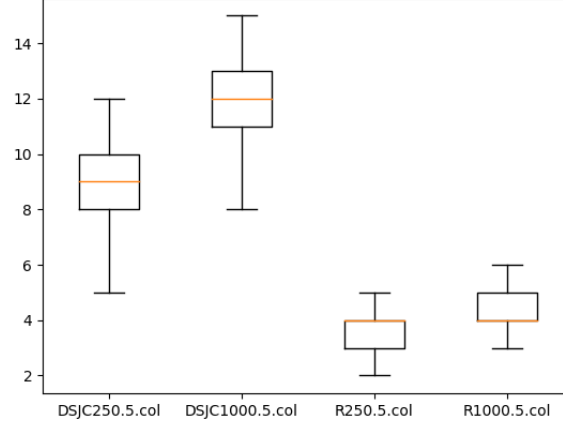


Fig. 8. Boxplot of the size distribution of the color groups in the solutions for graphs DSJC250.5.col, DSJC1000.5.col, R250.5.col and R1000.5.col colored by TensCol with 28, 84, 65 and 234 colors, respectively.

758 TensCol does not explore (large) shared color groups during the search. In-
759 stead, it inherits and learns *pairwise* information via the computation of the
760 *group concentration matrix* \tilde{M} with equation (4). In this matrix \tilde{M} , each en-
761 try (i, j) indicates the number of candidate solutions with vertices v_i and v_j
762 being assigned to the same color group. This pairwise information sharing
763 contributes to satisfactorily coloring geometric graphs. On the other hand, it
764 seems to be a disadvantage when dealing with large random graphics (since it
765 does not inherit large shared color groups).

766 This *pairwise* information sharing strategy is in sharp contrast to the refer-
767 ence algorithms that rely on recombination of large color groups (such as MA
768 and HEAD with the Greedy Partition Crossover (GPX) of [18]). These algo-
769 rithms are expected to perform well when large shared color groups are parts
770 of a solution (this is the case for random graphs such as DSJC250.5.col and
771 DSJC1000.5.col) and may fail if this condition is not met as for the geomet-
772 ric graphs such as R250.5.col and R1000.5.col. Indeed, an inspection of elite
773 candidate solutions (with conflicts) from the HEAD algorithm for coloring
774 R1000.5.col with $k = 234$ showed that the shared color groups inherited from
775 parent solutions include at least 7 vertices, while the largest color group in
776 legal 234-colorings has 6 vertices only. This indicates that memetic algorithms
777 with the GPX crossover (such as MA and HEAD) can be misguided by the
778 recombination, thus leading to mediocre results for this geometric graph.

⁷ Let us note that the fact that large color groups are not part of any optimal 234-coloring for the R1000.5.col instance was also observed in [43].

779 These discussions lead to the conclusion that TensCol can be considered as a
780 complementary approach with respect to the existing approaches, especially,
781 the memetic approach.

782 5.5.2 Analysis of the equitable coloring results

783 TensCol has attained a very good performance on many instances for the ECP,
784 including 8 new record-breaking results. TensCol seems powerful in finding
785 solutions with homogeneous sizes of color groups for the GCP, this may explain
786 its good results for the ECP. Indeed, given the equity constraint, the color
787 graphs of a solution for the ECP are necessarily of homogeneous sizes.

788 However TensCol also reported bad results (see Table 7) for some specific in-
789 stances, in particular for the wapXXa.col graphs. Two reasons can be advanced
790 to explain this counter-performance.

791 First, most of the wapXXa.col graphs are very large with more than 2000
792 vertices. Processing such a large graph by TensCol with $D = 200$ solutions
793 evaluated in parallel requires more than 16 Go on the GPU devices, surpassing
794 the memory limit of the computer used in this work. Therefore it was necessary
795 to reduce the number of candidate solutions evaluated at the same time to
796 $D = 20$, which impacts negatively the performance of the TensCol algorithm.

797 Second, most of the wapXXa.col instances present a very low density of edges
798 (between 2% and 8%) with a high number of vertices. Therefore the number
799 k of colors required to color these graphs is very low compared to the number
800 n of vertices (for the instance wap01a.col, the number of vertices is $n = 2368$
801 and the best coloring found in the literature only requires $k = 42$ colors).
802 It was empirically noticed that the gradient descent used by TensCol is less
803 informative in this case because the number of weights updated ($n \times k$) at each
804 iteration of the algorithm is reduced. In fact, TensCol benefits less from one of
805 its main advantages which is to encode information on the possible colors for
806 each vertex. In the extreme case of binary group assignment, with only two
807 weights per vertex, our weight learning strategy is expected to be less effective
808 compared to other approaches. This is consistent with the presented results
809 that TensCol is more effective for large graphs with a high number of groups
810 such as R1000.5, C2000.5 and C2000.9 colored with 239, 172 and 431 colors
811 (see Tables 6 and 8).

812 6 Other applications of the proposed method

813 In this section the generality of the proposed approach is discussed by showing
814 how it can be conveniently applied to solve other graph problems such as
815 multicoloring, minimum sum coloring and k -partitioning.

816 In the multicoloring problem [21], each vertex $v_i \in V$ is allocated a weight
817 $c_i \in \{1, 2, \dots\}$ and the task is to assign c_i different colors to each vertex v_i such
818 that adjacent vertices have no colors in common and the number of colors
819 used is minimal. For this problem, as c_i different colors have to be assigned to
820 each vertex, a modification has to be done in the vertex to color assignment
821 procedure of the TensCol algorithm (Step 1). Instead of selecting for the i -th
822 vertex the color group with the maximum weight in w_i , a set of c_i color groups
823 corresponding to the c_i maximum values of w_i could be selected.

824 In the minimum sum coloring problem [24], a weight z_l is associated with
825 each color and the objective is to find a legal coloring which minimizes the
826 sum of the total color cost. The TensCol algorithm could be used by replacing
827 the equity fitness $f_{eq}(S_d)$ in Algorithm 1 for each candidate solution by the
828 additive fitness $f_{mscp}(S_d) = \sum_{i=1}^n \sum_{l=1}^k s_{d,i,l} \times z_l$ corresponding to the sum of
829 the total color cost of a candidate solution S_d .

830 For the popular k -partitioning problem [14], the same TensCol algorithm could
831 be used except that M would be replaced by $\bar{M} = J - M$, where J is the
832 matrix of ones of size $n \times n$. Then, the fitness of a candidate solution for the k -
833 partitioning problem can be evaluated by $f(S_d) = \frac{1}{2} \text{sum}(A \odot \bar{M})$, corresponding
834 to the number of cut edges between partitions. For the k -partitioning variant
835 with a balancing constraint [1], the same additional *equity fitness* $f_{eq}(S_d)$ of
836 a candidate solution S_d given by equation (3) for the ECP could be added to
837 the fitness function of the graph partitioning problem.

838 7 Conclusion

839 A population-based gradient descent weight learning approach is presented in
840 this paper, as well as a practical implementation on GPU devices to solve graph
841 coloring problems. This approach has the particular feature of being general
842 and can be applied to different coloring (and other) problems with a suitable
843 global loss function. This is in sharp contrast to existing approaches for graph
844 coloring, which are specific to a problem. The proposed approach formulates
845 the computation of a solution as a weight tensor optimization problem which
846 is solved by a first order gradient descent. As such it can take advantage of
847 GPU accelerated training to deal with multiple parallel solution evaluations.

848 The proposed approach was assessed on the well-known graph coloring prob-
 849 lem and the related equitable coloring problem. The results of extensive exper-
 850 imental evaluations on popular DIMACS and COLOR02 challenge benchmark
 851 graphs showed that TensCol competes globally well with the best algorithms
 852 for both problems with an unified approach. Overall, even if TensCol does not
 853 find new record results for the GCP (this rarely happened since 2012), it pro-
 854 vides good results in particular for large geometric graphs (such as R1000.5.col
 855 or latin_square_10.col) which are particularly difficult for the best performing
 856 memetic algorithms. For the ECP, our method discovered 8 improved best
 857 results (new upper bounds) for large geometric graphs and random graphs,
 858 while the improvements for several graphs are very important in terms of the
 859 number of gained colors. Given the novelty of the approach and its promising
 860 results reached, this work can serve as the starting point for new research
 861 to further advance the state-of-the-art on solving graph coloring and other
 862 related problems as discussed in the last section.

863 A detailed analysis of the achieved results reveals however three main limita-
 864 tions of the proposed algorithm. First, the TensCol algorithm can be sensitive
 865 to its parameters for specific instances, especially regarding the ρ and λ pa-
 866 rameters. An adaptive strategy could be employed to adjust these parameters
 867 depending on the graph encountered [23]. Second, due to the memory ca-
 868 pacity of the GPU devices used for our experiments, TensCol has troubles
 869 to deal with very large graphs with more than 2000 vertices. This situation
 870 will change because GPU devices with much more memory are expected to
 871 become increasingly affordable in the coming years. Third, TensCol does not
 872 learn information about large shared color groups like the best performing
 873 memetic algorithms do with the GPX-like crossover. This partially explains
 874 the mediocre results of TensCol on some random instances of the GCP. It
 875 would be interesting to extend the TensCol algorithm to take into account
 876 group information. However, this feature also proves to be an advantage to
 877 deal with large geometric graphs for the GCP and for the ECP where the eq-
 878 uity constraint is imposed. TensCol can therefore be seen as a complementary
 879 approach with respect to the best existing approaches based on the memetic
 880 framework for graph coloring problems.

881 Other future works could be performed, but are not limited to the following.
 882 It would be interesting to test the proposed approach on other graph problems
 883 including those mentioned in Section 6. Furthermore, the optimization process
 884 of the learned weight tensor can be improved by using more sophisticated
 885 methods such as second order gradient descent with Hessian tensor, adaptive
 886 learning rate or momentum [6]. To learn more complex dependencies between
 887 the group assignments, it would be worth investigating advanced strategies
 888 to replace the weight tensor of candidate solutions by a product of tensors or
 889 even a deep generative neural network [3].

890 Finally, the two coloring problems studied in this work are general models that
891 can be used to formulate a number of real applications, such as scheduling and
892 timetabling (see the book [27] for more application examples). The algorithm
893 presented in this work could be adopted by researchers and practitioners to
894 solve such real problems. The availability of the source code of our algorithm
895 will further facilitate such applications.

896 Declaration of competing interest

897 The authors declare that they have no known competing financial interests or
898 personal relationships that could have appeared to influence the work reported
899 in this paper.

900 Acknowledgments

901 We are grateful to the reviewers for their useful comments and suggestions
902 which helped us to significantly improve the paper. This work was granted
903 access to the HPC resources of IDRIS under the allocation 2019-AD011011161
904 made by GENCI (French national supercomputing facility).

905 References

- 906 [1] Konstantin Andreev and Harald Racke. Balanced graph partitioning. *Theory*
907 *of Computing Systems*, 39(6):929–939, 2006.
- 908 [2] Takuya Aoki, Claus Aranha, and Hitoshi Kanoh. Pso algorithm with transition
909 probability based on hamming distance for graph coloring problem. In *2015*
910 *IEEE International Conference on Systems, Man, and Cybernetics*, pages 1956–
911 1961, 2015.
- 912 [3] Yoshua Bengio, Eric Laufer, Guillaume Alain, and Jason Yosinski. Deep
913 generative stochastic networks trainable by backprop. In *International*
914 *Conference on Machine Learning*, pages 226–234, 2014.
- 915 [4] Yoshua Bengio, Nicholas Léonard, and Aaron Courville. Estimating or
916 propagating gradients through stochastic neurons for conditional computation.
917 *arXiv preprint arXiv:1308.3432*, 2013.
- 918 [5] Meriem Bensouyad and Djamel-Eddine Saïdouni. A discrete flower pollination
919 algorithm for graph coloring problem. In *2nd IEEE International Conference*
920 *on Cybernetics 2015, Gdynia, Poland, June 24-26, 2015*, pages 151–155. IEEE,
921 2015.

- 922 [6] Dimitri P Bertsekas. *Convex Optimization Algorithms*. Athena Scientific
923 Belmont, 2015.
- 924 [7] John S Bridle. Training stochastic model recognition algorithms as networks can
925 lead to maximum mutual information estimation of parameters. In *Advances*
926 *in Neural Information Processing Systems*, pages 211–217, 1990.
- 927 [8] Peter Bugata and Peter Drotár. Weighted nearest neighbors feature selection.
928 *Knowledge-Based Systems*, 163:749–761, 2019.
- 929 [9] Thang Nguyen Bui, ThanhVu H. Nguyen, Chirag M. Patel, and Kim-Anh T.
930 Phan. An ant-based algorithm for coloring graphs. *Discrete Applied*
931 *Mathematics*, 156(2):190–200, 2008.
- 932 [10] Kui Chen and Hitoshi Kanoh. A discrete firefly algorithm based on similarity
933 for graph coloring problems. In Teruhisa Hochin, Hiroaki Hirata, and
934 Hiroki Nomiya, editors, *18th IEEE/ACIS International Conference on Software*
935 *Engineering, Artificial Intelligence, Networking and Parallel/Distributed*
936 *Computing, SNPD 2017, Kanazawa, Japan, June 26-28, 2017*, pages 65–70.
937 IEEE Computer Society, 2017.
- 938 [11] Daniele Costa and Alain Hertz. Ants can colour graphs. *Journal of the*
939 *Operational Research Society*, 48(3):295–305, 1997.
- 940 [12] Isabel Méndez Díaz, Graciela Nasini, and Daniel Severín. A tabu search
941 heuristic for the equitable coloring problem. In *International Symposium on*
942 *Combinatorial Optimization*, pages 347–358. Springer, 2014.
- 943 [13] Emanuel Falkenauer. *Genetic Algorithms and Grouping Problems*. John Wiley
944 & Sons, Inc., 1998.
- 945 [14] Per-Olof Fjällström. *Algorithms for graph partitioning: A survey*, volume 3.
946 Linköping University Electronic Press Linköping, 1998.
- 947 [15] Charles Fleurent and Jacques A Ferland. Genetic and hybrid algorithms for
948 graph coloring. *Annals of Operations Research*, 63(3):437–461, 1996.
- 949 [16] Hanna Furmańczyk and Marek Kubale. The complexity of equitable vertex
950 coloring of graphs. *Journal of Applied Computer Science*, 13(2):95–106, 2005.
- 951 [17] Philippe Galinier, Jean-Philippe Hamiez, Jin-Kao Hao, and Daniel Porumbel.
952 Recent advances in graph vertex coloring. In *Handbook of Optimization*, pages
953 505–528. Springer, 2013.
- 954 [18] Philippe Galinier and Jin-Kao Hao. Hybrid evolutionary algorithms for graph
955 coloring. *Journal of Combinatorial Optimization*, 3(4):379–397, 1999.
- 956 [19] Philippe Galinier and Alain Hertz. A survey of local search methods for graph
957 coloring. *Computers & Operations Research*, 33(9):2547–2562, 2006.
- 958 [20] Michael R Garey and David S Johnson. *Computers and Intractability: A Guide*
959 *to the Theory of NP-Completeness*. WH Freeman, San Francisco, New York,
960 USA, 1979.

- [21] Magnús M Halldórsson and Guy Kortsarz. Multicoloring: Problems and techniques. In *International Symposium on Mathematical Foundations of Computer Science*, pages 25–41. Springer, 2004.
- [22] Alain Hertz and Dominique de Werra. Using tabu search techniques for graph coloring. *Computing*, 39(4):345–351, 1987.
- [23] Changwu Huang, Yuanxiang Li, and Xin Yao. A survey of automatic parameter tuning methods for metaheuristics. *IEEE Transactions on Evolutionary Computation*, 24(2):201–216, 2020.
- [24] Yan Jin, Jean-Philippe Hamiez, and Jin-Kao Hao. Algorithms for the minimum sum coloring problem: a review. *Artificial Intelligence Review*, 47(3):367–394, 2017.
- [25] Xiangjing Lai, Jin-Kao Hao, and Fred Glover. Backtracking based iterated tabu search for equitable coloring. *Engineering Applications of Artificial Intelligence*, 46:269–278, 2015.
- [26] Yann LeCun, Bernhard Boser, John S Denker, Donnie Henderson, Richard E Howard, Wayne Hubbard, and Lawrence D Jackel. Backpropagation applied to handwritten zip code recognition. *Neural Computation*, 1(4):541–551, 1989.
- [27] Rhyd Lewis. *A Guide to Graph Colouring - Algorithms and Applications*. Springer, 2016.
- [28] Zhipeng Lü and Jin-Kao Hao. A memetic algorithm for graph coloring. *European Journal of Operational Research*, 203(1):241–250, 2010.
- [29] Shadi Mahmoudi and Shahriar Lotfi. Modified cuckoo optimization algorithm (MCOA) to solve graph coloring problem. *Applied Soft Computing*, 33:48–64, 2015.
- [30] Enrico Malaguti, Michele Monaci, and Paolo Toth. A metaheuristic approach for the vertex coloring problem. *INFORMS Journal on Computing*, 20(2):302–316, 2008.
- [31] Enrico Malaguti, Michele Monaci, and Paolo Toth. An exact approach for the vertex coloring problem. *Discrete Optimization*, 8(2):174–190, 2011.
- [32] Enrico Malaguti and Paolo Toth. A survey on vertex coloring problems. *International Transactions in Operational Research*, 17(1):1–34, 2010.
- [33] Isabel Méndez-Díaz, Graciela Nasini, and Daniel Severín. A dsatur-based algorithm for the equitable coloring problem. *Computers & Operations Research*, 57:41–50, 2015.
- [34] Walter Meyer. Equitable coloring. *The American Mathematical Monthly*, 80(8):920–922, 1973.
- [35] Laurent Moalic and Alexandre Gondran. Variations on memetic algorithms for graph coloring problems. *Journal of Heuristics*, 24(1):1–24, 2018.

- 999 [36] Ferrante Neri, Carlos Cotta, and Pablo Moscato, editors. *Handbook of Memetic*
1000 *Algorithms*, volume 379 of *Studies in Computational Intelligence*. Springer,
1001 2012.
- 1002 [37] David E Rumelhart, Geoffrey E Hinton, and Ronald J Williams. Learning
1003 internal representations by error propagation. Technical report, California Univ
1004 San Diego La Jolla Inst for Cognitive Science, 1985.
- 1005 [38] Dimitris Spathis, Nikolaos Passalis, and Anastasios Tefas. Interactive
1006 dimensionality reduction using similarity projections. *Knowledge-Based*
1007 *Systems*, 165:77–91, 2019.
- 1008 [39] Wen Sun, Jin-Kao Hao, Xiangjing Lai, and Qinghua Wu. On feasible and
1009 infeasible search for equitable graph coloring. In *Proceedings of the Genetic*
1010 *and Evolutionary Computation Conference*, pages 369–376. ACM, 2017.
- 1011 [40] Wen Sun, Jin-Kao Hao, Wenyu Wang, and Qinghua Wu. Memetic search for
1012 the equitable coloring problem. *Knowledge-Based Systems*, 188:105000, 2020.
- 1013 [41] Olawale Titiloye and Alan Crispin. Quantum annealing of the graph coloring
1014 problem. *Discrete Optimization*, 8(2):376–384, 2011.
- 1015 [42] Wenyu Wang, Jin-Kao Hao, and Qinghua Wu. Tabu search with feasible and
1016 infeasible searches for equitable coloring. *Engineering Applications of Artificial*
1017 *Intelligence*, 71:1–14, 2018.
- 1018 [43] Qinghua Wu and Jin-Kao Hao. Coloring large graphs based on independent set
1019 extraction. *Computers & Operations Research*, 39(2):283–290, 2012.
- 1020 [44] Yangming Zhou, Béatrice Duval, and Jin-Kao Hao. Improving probability
1021 learning based local search for graph coloring. *Applied Soft Computing*, 65:542–
1022 553, 2018.
- 1023 [45] Yangming Zhou, Jin-Kao Hao, and Béatrice Duval. Reinforcement learning
1024 based local search for grouping problems: A case study on graph coloring. *Expert*
1025 *Systems with Applications*, 64:412–422, 2016.

1026 **Appendix - Comparative results of TensCol with state-of-the-art**
1027 **algorithms on the GCP and the ECP**

Table 4

Comparative results of TensCol with state-of-the-art algorithms on the set of 36 most difficult DIMACS graphs for the GCP (1/2). Numbers in bold indicate that the best result k_{best} found by the algorithm attains the overall best-known result in the literature k^* or the chromatic number.

Instance	V	$\chi(G)$	k^*	PLSCOL			MMT			MA			QA			HEAD		TensCol		
				k_{best}	SR	t(s)	k_{best}	SR	t(s)	k_{best}	SR	t(s)	k_{best}	SR	t(s)	k_{best}	SR		t(s)	
DSJC125.1	125	5	5	5	10/10	< 60	5	-	21	5	10/10	60	-	-	5	20/20	< 1	5	10/10	40
DSJC125.5	125	17	17	17	10/10	< 60	17	-	122	17	10/10	180	-	-	17	20/20	< 1	17	10/10	68
DSJC125.9	125	44	44	44	10/10	< 60	44	-	121	44	10/10	240	-	-	44	20/20	< 1	44	10/10	22
DSJC250.1	250	?	8	8	10/10	< 60	8	-	21	8	10/10	120	-	-	8	20/20	< 1	8	10/10	95
DSJC250.5	250	?	28	28	10/10	4	28	-	117	28	20/20	< 60	28	10/10	8	20/20	0.6	28	10/10	199
DSJC250.9	250	?	72	72	10/10	< 60	72	-	89	72	10/10	180	-	-	72	20/20	1.2	72	10/10	87
DSJC500.1	500	?	12	12	7/10	43	12	-	210	12	20/20	< 60	12	10/10	82	20/20	6	12	10/10	1098
DSJC500.5	500	?	47	48	3/10	1786	48	-	388	48	20/20	1320	48	10/10	494	2/10000	48	48	5/10	7807
DSJC500.9	500	?	126	126	10/10	747	127	-	433	126	20/20	5700	126	10/10	1198	13/20	72	126	6/10	18433
DSJC1000.1	1000	?	20	20	1/10	3694	20	-	260	20	16/20	6480	20	9/10	2842	20/20	12	20	10/10	10225
DSJC1000.5	1000	?	82	87	10/10	1419	84	-	8407	83	20/20	2820	83	9/10	12773	3/20	2880	84	9/10	32495
DSJC1000.9	1000	?	222	223	5/10	12094	225	-	3234	223	18/20	9000	222	2/10	13740	2/20	5160	224	6/10	58084
DSJR500.1	500	12	12	12	10/10	< 60	12	-	25	12	10/10	240	-	-	-	-	-	12	10/10	7
DSJR500.1c	500	?	85	85	10/10	386	85	-	88	85	20/20	300	85	10/10	525	1/20	12	85	10/10	298
DSJR500.5	500	?	122	126	8/10	1860	122	-	163	122	11/20	6900	122	2/10	370	-	-	122	10/10	4310
flat300.26.0	300	26	26	26	10/10	195	26	-	36	26	20/20	240	-	-	-	-	-	26	10/10	176
flat300.28.0	300	28	28	30	10/10	233	31	-	212	29	15/20	7680	31	10/10	19	20/20	1.2	31	10/10	586
flat1000.76.0	1000	76	81	86	1/10	5301	83	-	7325	82	20/20	4080	82	7/10	9802	3/20	3600	83	3/10	34349
latin_square.10	900	?	97	99	8/10	2005	101	-	5156	99	5/20	9480	98	10/10	1449	-	-	98	10/10	28925

Table 5

Comparative results of TensCol with state-of-the-art algorithms on the set of 36 most difficult DIMACS graphs for the GCP (2/2). Numbers in bold indicate that the best result k_{best} found by the algorithm attains the overall best-known result in the literature k^* or the chromatic number.

Instance	V	$\chi(G)$	k^*	PLSCOL			MMT			MA			QA			HEAD			TensCol		
				k_{best}	SR	t(s)	k_{best}	SR	t(s)	k_{best}	SR	t(s)	k_{best}	SR	t(s)	k_{best}	SR	t(s)	k_{best}	SR	t(s)
le450.15a	450	15	15	15	10/10	< 60	15	-	< 1	15	10/10	120	-	-	-	15	20/20	< 1	15	10/10	333
le450.15b	450	15	15	15	10/10	< 60	15	-	< 1	15	10/10	120	-	-	-	15	20/20	< 1	15	10/10	333
le450.15c	450	15	15	15	7/10	1718	15	-	3	15	20/20	180	-	-	-	15	20/20	1.2	15	10/10	507
le450.15d	450	15	15	15	3/10	2499	15	-	4	15	20/20	300	-	-	-	15	1/20	1.8	15	10/10	301
le450.25a	450	25	25	25	10/10	< 60	-	-	-	25	10/10	120	-	-	-	25	20/20	< 1	25	10/10	87
le450.25b	450	25	25	25	10/10	< 60	-	-	-	25	10/10	180	-	-	-	25	20/20	< 1	25	10/10	12
le450.25c	450	25	25	25	10/10	1296	25	-	1321	25	20/20	900	-	-	-	25	20/20	1800	25	10/10	19680
le450.25d	450	25	25	25	10/10	1704	25	-	436	25	20/20	600	-	-	-	25	20/20	5400	25	10/10	9549
R125.1	125	5	5	5	10/10	< 60	5	-	< 1	5	10/10	120	-	-	-	-	-	-	5	10/10	0.03
R125.5	125	36	36	36	10/10	< 60	36	-	21	36	-	< 1	36	10/10	60	-	-	-	36	10/10	6.2
R250.1	250	8	8	8	10/10	< 60	8	-	< 1	8	10/10	300	-	-	-	-	-	-	8	10/10	0.04
R250.5	250	65	65	66	10/10	705	65	-	64	65	20/20	240	65	9/10	168	65	1/20	780	65	10/10	33
R1000.1	1000	?	20	20	10/10	< 60	20	-	37	20	10/10	120	-	-	-	-	-	-	20	10/10	15
R1000.1c	1000	?	98	98	10/10	256	98	-	518	98	20/20	480	98	10/10	287	98	3/20	12	98	10/10	4707
R1000.5	1000	?	234	254	4/10	7818	234	-	753	238	13/20	16560	238	3/10	9511	245	20/20	14640	234	2/10	23692

Table 6

Comparative results of TensCol with state-of-the-art algorithms on the 73 benchmark ECP instances (1/4). Numbers in bold indicate that the best result k_{best} found by the algorithm is equal to the overall best-known result k^* in the literature. A star in column k_{best} for TensCol indicates that a new best coloring of the ECP has been found.

Instance	V	k^*	TabuEqCol			BITS			FISA			HTS			MAECP			TensCol		
			k_{best}	SR	t(s)	k_{best}	SR	t(s)	k_{best}	SR	t(s)	k_{best}	SR	t(s)	k_{best}	SR	t(s)	k_{best}	SR	t(s)
DSJC125.1	125	5	5	-	0.8	5	20/20	0.96	5	20/20	0.62	5	20/20	15.7	5	20/20	1.26	5	10/10	50
DSJC125.5	125	9	18	-	788	17	10/20	5169	17	20/20	428	17	20/20	563	17	19/20	2432	17	10/10	124
DSJC125.9	125	44	45	-	0.4	44	20/20	0.16	44	20/20	0.09	44	20/20	0.3	44	20/20	2.8	44	10/10	22
DSJC250.1	250	8	8	-	32	8	20/20	5.5	8	20/20	3.62	8	20/20	427	8	20/20	4.8	8	10/10	97
DSJC250.5	250	29	32	-	69	30	1/20	3265	29	13/20	5236	29	20/20	4584	29	20/20	1093	29	10/10	312
DSJC250.9	250	72	83	-	1.2	72	20/20	1180	72	20/20	892	72	20/20	1835	72	18/20	2540	72	9/10	1285
DSJC500.1	500	13	13	-	33	13	20/20	6.96	13	20/20	3.57	13	20/20	148	13	20/20	112.67	13	10/10	168
DSJC500.5	500	51	63	-	11	56	1/20	484	52	1/20	8197	52	20/20	2098	51	1/20	20784	51	10/10	3793
DSJC500.9	500	128	182	-	0.7	129	2/20	3556	130	3/20	6269	129	7/20	8926	128	2/20	16170	129	4/10	13537
DSJR500.1	500	12	12	-	0.0	12	20/20	0.58	12	20/20	0.38	12	20/20	2.53	12	20/20	13.9	12	10/10	490
DSJR500.5	500	124	133	-	0.1	126	14/20	3947	126	10/20	4459	125	7/20	8179	124	1/20	13266	122*	10/10	5021
DSJC1000.1	1000	21	22	-	500	21	1/20	3605	21	20/20	1866	21	1/20	4809	21	17/20	1365	21	9/10	1757
DSJC1000.5	1000	95	112	-	2261	103	3/20	18079	95	2/20	15698	95	6/20	13394	95	3/20	36321	92*	10/10	12430
DSJC1000.9	1000	251	329	-	20	252	1/20	4065	252	16/20	2240	251	20/20	3564	251	20/20	963	251	10/10	20862
R125.1	125	5	-	-	-	5	20/20	0.01	5	20/20	0	5	20/20	0.06	5	20/20	0.37	5	10/10	0.07
R125.5	36	36	-	-	-	36	20/20	0.39	36	20/20	0.67	36	20/20	3.41	36	20/20	1.76	36	10/10	29
R250.1	250	8	-	-	-	8	20/20	0.01	8	20/20	0	8	20/20	0.11	8	20/20	0.24	8	10/10	0.13
R250.5	250	65	-	-	-	66	7/20	6275	66	2/20	3041	65	2/20	9778	65	3/20	11291	65	10/10	40
R1000.1	1000	20	-	-	-	20	20/20	3.09	20	20/20	2.24	20	20/20	678	20	20/20	21	20	10/10	4426
R1000.5	1000	247	-	-	-	250	12/20	10723	250	11/20	11564	249	19/20	17817	247	3/20	11291	239*	9/10	53187

Table 7

Comparative results of TensCol with state-of-the-art algorithms on the 73 benchmark ECP instances (2/4). Numbers in bold indicate that the best result k_{best} found by the algorithm is equal to the overall best-known result k^* in the literature. A star in column k_{best} for TensCol indicates that a new best coloring of the ECP has been found.

Instance	V	k^*	TabuEqCol			BITS			FISA			HTS			MAECP			TensCol		
			k_{best}	SR	t(s)	k_{best}	SR	t(s)	k_{best}	SR	t(s)	k_{best}	SR	t(s)	k_{best}	SR	t(s)	k_{best}	SR	t(s)
le450_5a	450	5	-	-	-	5	20/20	46	5	20/20	30.2	5	20/20	332	5	20/20	38.4	5	10/10	15
le450_5b	450	5	7	-	7.2	5	20/20	74	5	20/20	44.29	5	20/20	364	5	20/20	64.7	5	10/10	22
le450_5c	450	5	-	-	-	5	20/20	1877	5	20/20	16.39	5	20/20	143	5	20/20	17.5	5	10/10	4
le450_5d	450	5	8	-	15	5	20/20	2231	5	20/20	14.07	5	20/20	373	5	20/20	16.1	5	10/10	3
le450_15a	450	15	-	-	-	15	20/20	4.44	15	20/20	2.99	15	20/20	17	15	20/20	7.4	18	10/10	4252
le450_15b	450	15	15	-	107	15	20/20	4.16	15	20/20	2.41	15	20/20	31664	15	20/20	8.0	18	10/10	3346
le450_15c	450	15	-	-	-	15	18/20	410	15	16/20	553	15	20/20	96	15	20/20	1351	15	10/10	120
le450_15d	450	15	16	-	599	15	6/20	629	15	3/20	638	15	20/20	58	15	13/20	4992	15	10/10	178
le450_25a	450	25	-	-	-	25	20/20	0.72	25	20/20	0.41	25	20/20	4.8	25	20/20	20.2	25	10/10	6343
le450_25b	450	25	25	-	0.0	25	20/20	0.78	25	20/20	0.46	25	20/20	7.3	25	20/20	28.1	25	10/10	2411
le450_25c	450	26	-	-	-	26	20/20	16.5	26	20/20	86.9	26	20/20	11.8	26	20/20	148	31	2/10	46129
le450_25d	450	26	27	-	29	26	20/20	14.08	26	20/20	95.9	26	20/20	6.3	26	20/20	61	31	10/10	33419
wap01a	2368	42	46	-	15	42	8/20	4183	42	1/20	4545	42	20/20	700	42	20/20	10304	46	2/10	1891
wap02a	2464	41	44	-	83	41	4/20	6829	41	2/20	2538	41	20/20	2233	41	20/20	14295	47	8/10	1657
wap03a	4730	44	50	-	464	45	19/20	11267	45	6/20	20202	45	18/20	6150	44	2/20	34445	51	2/10	5522
wap04a	5231	43	-	-	-	44	17/20	11345	44	11/20	15614	44	12/20	12845	43	2/20	33286	51	6/10	2376
wap05a	905	50	-	-	-	50	20/20	8.46	50	20/20	99.26	50	20/20	0.18	50	20/20	10983	50	10/10	417
wap06a	947	41	-	-	-	41	6/20	6892	41	1/20	9340	41	20/20	1206	41	19/20	13739	45	8/10	413
wap07a	1809	42	-	-	-	43	19/20	718	43	19/20	4077	42	12/20	2591	42	5/20	11304	49	10/10	995
wap08a	1870	42	-	-	-	43	19/20	951	43	10/20	4872	42	6/20	3801	42	18/20	13821	47	2/10	1171

Table 8

Comparative results of TensCol with state-of-the-art algorithms on the 73 benchmark ECP instances (3/4). Numbers in bold indicate that the best result k_{best} found by the algorithm is equal to the overall best-known result k^* in the literature. A star in column k_{best} for TensCol indicates that a new best coloring of the ECP has been found.

Instance	V	k^*	TabuEqCol			BITS			FISA			HTS			MAECP			TensCol		
			k_{best}	SR	t(s)	k_{best}	SR	t(s)	k_{best}	SR	t(s)	k_{best}	SR	t(s)	k_{best}	SR	t(s)	k_{best}	SR	t(s)
flat300_28.0	300	32	36	-	3222	34	6/20	4407	32	1/20	4910	33	20/20	3801	32	7/20	5209	32	10/10	1583
flat1000_50.0	1000	92	-	-	-	101	1/20	9206	94	6/20	17321	92	1/20	18035	93	2/20	16779	92	7/10	5566
flat1000_60.0	1000	93	-	-	-	102	5/20	10201	94	5/20	10489	94	8/20	16263	93	3/20	14715	92*	10/10	5905
flat1000_76.0	1000	93	112	-	1572	102	3/20	13063	94	2/20	15246	93	5/20	14307	93	2/20	24103	91*	3/10	53553
latin_square_10	900	103	130	-	1301	115	1/20	17859	104	10/20	12666	107	3/20	18055	103	1/20	32403	103	8/10	37233
C2000.5	2000	183	-	-	-	201	7/20	4808	183	13/20	19702	188	1/20	19915	183	20/20	4555	102*	1/10	14484
C2000.9	2000	468	-	-	-	502	11/20	7772	493	2/20	21164	501	20/20	3952	468	1/20	36966	172*	8/10	111884
multsol.i.1	197	49	50	-	0.0	49	20/20	14.82	49	20/20	44.34	49	20/20	0.53	49	20/20	7.9	431*	4/10	109243
multsol.i.2	188	36	48	-	0.1	36	13/20	3633	36	2/20	1914	36	20/20	15	36	20/20	188	49	10/10	301
fpsol2.i.1	496	65	78	-	0.1	65	20/20	8302	65	20/20	1723	65	20/20	12.61	65	20/20	777	36	3/10	2877
fpsol2.i.2	451	47	60	-	0.0	47	20/20	976	47	17/20	2357	47	20/20	6.64	47	20/20	4983	65	10/10	3033
fpsol2.i.3	425	55	79	-	0.0	55	20/20	729	55	20/20	1310	55	20/20	3.77	55	20/20	746	47	10/10	1725
inithx.i.1	864	54	66	-	0.1	54	20/20	1468	54	7/20	3356	54	20/20	47.3	54	20/20	1708	55	10/10	135
inithx.i.2	645	35	93	-	7.2	36	13/20	12412	36	5/20	3275	35	20/20	207.4	35	20/20	4106	54	9/10	11620
inithx.i.3	621	36	-	-	-	37	11/20	9214	37	4/20	2891	36	20/20	5256	36	20/20	6529	35	10/10	3039
zerosin.i.1	211	49	51	-	0.0	49	20/20	1367	49	8/20	1089	49	20/20	2.24	49	7/20	5749	36	10/10	4943
zerosin.i.2	211	36	51	-	0.0	36	20/20	97	36	20/20	124	36	20/20	0.7	36	20/20	66.7	49	10/10	449
zerosin.i.3	206	36	49	-	0.0	36	20/20	109	36	20/20	129	36	20/20	1.14	36	20/20	166	36	10/10	66
myciel6	95	7	7	-	0.0	7	20/20	0.0	7	20/20	0	7	20/20	0.01	7	20/20	0.56	36	10/10	65
myciel7	191	8	8	-	0.1	8	20/20	0.02	8	20/20	0.02	8	20/20	0.17	8	20/20	1.81	7	10/10	5

Table 9

Comparative results of TensCol with state-of-the-art algorithms on the 73 benchmark ECP instances (4/4). Numbers in bold indicate that the best result k_{best} found by the algorithm is equal to the overall best-known result k^* in the literature. A star in column k_{best} for TensCol indicates that a new best coloring of the ECP has been found.

Instance	V	TabuEqCol			BITS			FISA			HTS			MAECP			TensCol		
		k_{best}	SR	t(s)	k_{best}	SR	t(s)	k_{best}	SR	t(s)	k_{best}	SR	t(s)	k_{best}	SR	t(s)	k_{best}	SR	t(s)
4_FullIns_3	114	7	-	0.1	7	20/20	0.0	7	20/20	0	7	20/20	0.01	7	20/20	0	7	10/10	10
4_FullIns_4	690	8	-	0.4	8	20/20	0.23	8	20/20	0.12	8	20/20	3.98	8	20/20	2.36	8	10/10	26
4_FullIns_5	4146	9	-	254	9	20/20	54.49	9	20/20	0.12	9	14/20	57.7	9	20/20	72.5	9	10/10	5191
1_Insertions_6	607	7	-	0.2	7	20/20	0.34	7	20/20	0.17	7	20/20	0.38	7	20/20	4.61	7	10/10	20
2_Insertions_5	597	6	-	0.0	6	20/20	0.11	6	20/20	0.06	6	20/20	0.96	6	20/20	1.22	6	10/10	17
3_Insertions_5	1406	6	-	1.2	6	20/20	0.57	6	20/20	0.35	6	20/20	21.94	6	20/20	2.77	6	10/10	641
schooll	385	15	-	12	15	20/20	1.3	15	20/20	0.93	15	20/20	0.72	15	20/20	9.17	15	10/10	16
schooll_nsh	352	14	-	14	20/20	2.63	14	20/20	1.77	14	20/20	56.1	14	14	20/20	17.3	14	8/10	1181
qg.order40	1600	40	-	47	40	20/20	4.73	40	20/20	3.44	40	20/20	4291	40	20/20	1627	40	10/10	44
qg.order60	3600	60	-	267	60	20/20	21.57	60	20/20	14.53	60	20/20	64.3	60	20/20	1015	60	10/10	655
ash331GPIA	662	4	-	2	4	20/20	2.02	4	20/20	0.78	4	20/20	5.39	4	20/20	43.8	4	10/10	554
ash608GPIA	1216	4	-	12	4	20/20	0.5	4	20/20	0.25	4	20/20	854	4	20/20	0.44	4	9/10	749
ash958GPIA	1916	4	-	41	4	20/20	23.31	4	20/20	10.89	4	20/20	11.95	4	20/20	166	4	4/10	2819